Exploring Robust Interactions Between Human Intention and Inanimate/Animate Systems

By

William A. Tiller, Walter E. Dibble, Jr. and Michael J. Kohane

ABSTRACT

Based on the present paradigm, the conventional viewpoint is that humans cannot meaningfully interact, via their intention, with target experiments. Even more strongly, one would state that human intention cannot possibly be captured in a simple electronic device and then have the device meaningfully interact with target experiments.

Over the course of the past two years, the authors have conducted three very different target experiments using Intention Imprinted Electronic Devices (IIED's) and found robust interaction between these simple devices and the target experiments in complete opposition to the view of the prevailing paradigm.

On the experimental side, for each target experiment one starts with two identical physical devices, isolates one from the other and "charges" one with the specific intention for the particular experiment. This charging process involved the services of four highly qualified meditators to imprint the device with the specific intention. The devices with the same imprint were then wrapped in Al foil and stored in an electrically grounded Faraday cage until the next step in the process. Next, when needed, the Al-foil wrapped devices were separately shipped, via Federal Express, to their laboratory destination about 2000 miles away. On arriving there, they were immediately placed in separate, grounded Faraday cages until use in the actual target experiments conducted by others.

For the three target experiments, the general intentions were (1) to decrease (increase) the pH of water by one pH unit, (2) to increase the ATP/ADP ratio in fruit fly larvae so as to significantly decrease the larval development time

and (3) to significantly increase the thermodynamic activity of the specific liver enzyme, alkaline phosphatase (ALP). For target experiment (1) changes of ≈ 0.5 to 1.0 pH units increase or decrease, with a measurement accuracy of ∓ 0.01 pH units, was achieved. For target experiment (2), reductions of ≈ 15 % in larval development time for the imprinted vs. unimprinted device were observed ($p < 0.001$). For target experiment (3), increases in thermodynamic activity for ALP of ≈ 10 % to 20 % were achieved ($p < 0.001$).

In pure water containing small solid particles, pH oscillations of both short (≈ 1 hour) and long (≈ 20 hour) period were observed. In multiple vessel studies with the IIED located only near one vessel, the following was observed, (a) a strong correlation in pH-oscillation behavior between the IIED-vessel and other simultaneously pH-monitored vessels located ≈ 115 feet to 155 feet distant, (b) a location-specific conditioning behavior associated with repeated running of the target experiment day after day at that specific location and (c) the presence of temperature oscillations in-phase with the pH-oscillations in the vessels. Fourier transforms of the various real-time plots were utilized to quantify the correlations.

In this paper, we also address many of the issues associated with (1) the device imprinting procedures, (2) the effective isolation of imprinted and unimprinted devices, (3) retention time for the "intention charge", (4) conditioning of the experimental site, (5) the necessary and sufficient set of experimental protocols needed to assure repeatability of our results by others, (6) a multidimensional theoretical model for rationalizing these observations, (7) the philosophical significance of these results to an evolving humanity and (8) the relevance of these results to consciousness studies.

Exploring Robust Interactions Between Human Intention and Inanimate/Animate Systems

by

William A. Tiller, Walter E. Dibble, Jr. and Michael J. Kohane

Introduction

The prevailing paradigm for science and technology is that focussed human intention cannot meaningfully interact, at an energy/information level, with specific target experiments and even less so via an intermediary electronic device. Abundant historical technological and present day experience with expert systems, computer-aided design, etc., buttresses this viewpoint. This has led humanity down a reductionist and materialistic path. On the other hand, one can certainly conceive of a society whose consciousness is sufficiently developed that their focussed intentions would robustly influence specific target experiments. Such a condition would require the development of a new paradigm and would indicate that a significant transformation had occurred in the human species. Such a species would further evolve down a very different path.

Over the course of the past two years, the authors have conducted three very different target experiments using intention imprinted electronic devices (IIED's) and found robust interaction between these simple devices and the target experiments in complete opposition to the view of the prevailing paradigm. Whether or not this indicates a cosmological change, destined to move humanity towards this alternate path of evolution, it is too early to say. However, it seems clear that consciousness-directed intention must be incorporated into any new paradigm and that is the overview focus of this paper. This paper

is a review of much of our recent experimental and theoretical work on this subject [1-9], the majority of it being in various stages of publication at the moment.

On the experimental side, for each target experiment, one starts with two identical physical devices, isolates them from each other and "charges" one with the specific intention for the particular experiment. This charging process involved the services of four highly qualified meditators to imprint the device with the specific intention. The devices with the same imprint were then wrapped in aluminum foil and stored in an electrically grounded Faraday cage until the next step in the process. Next, when needed, the aluminum foil wrapped devices were separately shipped, via Federal Express, to their laboratory destination ~2000 miles away. On arriving there, they were immediately placed in separate, grounded Faraday cages until use in the actual target experiments conducted by others.

For the three experiments, the intentions were (1) to decrease (increase) the pH of water by one pH unit, (2) to increase the ATP/ADP ratio in fruit fly larvae so as to significantly decrease their development time and (3) to significantly increase the thermodynamic activity of the specific liver enzyme, ALP. For (1), changes of 0.5 to 1.0 pH units were achieved [4] while, for (2), reductions of ~ 15% in larval development time for the imprinted vs. unimprinted device were observed ($p < 0.001$) [5] and, for (3), increases in thermodynamic activity of ~ 10% - 20% were achieved ($p < 0.001$) [7]. Further, in subsequent water plus small particulate solutions, pH-oscillations of both short and long period were observed. In multiple vessel studies with the IIED located only near one vessel, the following was observed (a) strong correlation of pH-oscillation behavior between the IIED-vessel and other monitored vessels located ~ 115 ft. to 155 ft. distant, (b) a location-conditioning behavior associated with repeated running of the experiment day after day and (c) the presence of temperature-oscillations correlated with the pH-oscillations [6]. All of

these observations point to the presence of a time-dependent pattern of coherence that develops in the water in association with the use of an IIED in the "on" state [4].

In this paper, we also address many of the issues associated with (1) the device imprinting procedures, (2) effective isolation of imprinted and unimprinted devices, (3) retention time of intention charge, (4) conditioning of the experimental site, (5) the necessary and sufficient set of experimental conditions needed to assure repeatability of our results by others, (6) a theoretical basis for understanding, or at least rationalizing, these experimental observations and (7) the philosophical significance of these results for evolving humanity.

Experimental Procedures

In each of the target experiments, two physically identical devices were used but one was imprinted with human intention while the other was not. The physical size of the plastic case housing the electronics is ~ 7 in. x 3 in. x 1 in. The electric circuits utilized are quite simple as can be seen from figure 1. They basically involve only an E PROM memory component, an oscillator component (1-10 MHz range), no intentional antenna and either line voltage or battery power supply. The radiated electrical power is less than ~ 1 μ watt at a distance of ~ 3 in. Both the unimprinted and imprinted devices were individually wrapped in aluminum foil and separately stored in individual electrically grounded Faraday cages for energy/information isolation purposes. They were taken out and unwrapped only for use in their target experiment and then re-wrapped and returned to their own Faraday cage until their next test.

The actual imprinting procedure for a particular target experiment was as follows: (a) place both the single-oscillator and the three oscillator devices along with their current

transformers on a table around which the imprinters sit, (b) four people (two men plus two women) who were all accomplished meditators, coherent, inner self-managed and readily capable of entering an ordered mode of heart function plus sustaining it for an extended period of time, sat around the table ready to enter a deep meditative state, (c) a signal was then given to enter such an internal state, to cleanse the environment and create a sacred space for the intention. Then, a signal was given by one of the four to put attention on the table-top objects and begin a mental cleansing process to erase any prior imprints from the devices, (d) after 3 or 4 minutes, another signal was given to begin focussing on the specific prearranged intention statement for about 10-15 minutes, (e) next, a final signal was given to shift focus to a closing intention designed to seal the imprint into the devices and minimize leakage of this essential energy/information from the devices. This completed the process so the four people withdrew from the meditative state and returned to their normal state of consciousness.

It should be obvious to the reader that a wide variety of options and variants exist with respect to the erasing, imprinting and sealing phases of the overall treatment process for these devices. The specific intentions used for the three target experiments reported on here are:

1. Water Experiment: To activate the indwelling consciousness of the system so that the IIED decreases (or increases) the pH of the experimental water by one pH unit compared to the control; i.e., increase (or decrease) the H^+ content of this water by a factor of 10.

2. Fruit Fly Experiment: To synergistically influence (a) the availability of oxygen, protons and ADP (adenine diphosphate) and (b) the activity of the available concentration of NAD (nicotinamide adenine dinucleotide) plus the activity of the available enzymes, dehydrogenase and ATP-synthase in the mitochondria so that the production of ATP

(adenine triphosphate) in the fruit fly larvae is significantly increased (as much as possible without harming the life function) relative to that of the control sample.

3. Enzyme Experiment: To activate the indwelling consciousness of the devices so as to increase by a significant factor (as much as possible), the thermodynamic activity coefficient of the specific liver enzyme, alkaline phosphatase. This activity coefficient increase is to occur relative to the same type of experiment conducted with unimprinted devices.

A. Water Target Experiment: Figure 2 provides a schematic illustration of the equipment involved in the pH measurement system. An Accumet 50 pH meter was utilized with fast-response, high performance, combination electrodes with automatic temperature compensation. The measurement accuracy was ±0.01 pH unit while calibration involved the use of buffer standards, pH 4, pH 7 and pH 10 (two of these were used depending on the pH of the solution). Measurements were made by placing the electrode in unstirred solution and recording the pH-time variation until a stable value was approached.

The four waters utilized in these experiments were (a) commercial bottled Evian water which is a Ca/Mg bicarbonate solution of initial pH = 7.00 with total dissolved solids of 300 mg/l and $[Ca^{++}]/[Mg^{++}] = 3.2$; (b) commercial bottled Castle Rock water, which is also a Ca/Mg bicarbonate solution of initial pH = 7.10, total dissolved solids of 95 mg/l and $[Ca^{++}]/[Mg^{++}] = 2.0$. This water was diluted 50/50 with ASTM type I purified water to ensure that no Ca/Mg carbonates precipitated during the course of the experiments; (c) ASTM Type I purified water and (d) ASTM type I purified water containing 4 gm/l of fine $ZnCO_3$ crystallites (~ a little larger than typical colloid size). After sample preparation, the solution was poured into several polypropylene bottles, with at least one always saved as a control. For storage and awaiting testing, bottles with any variation in their history were placed in

their own electrically grounded Faraday cage constructed from a fine mesh copper screen (0.16" grid).

The earliest experiments were conducted with the Evian water and took place at Stanford University. Because we didn't know much about what to expect, the water was treated with the device in one building and then walked ~ 150 feet to another building for measurement. It was thought that separation of the two steps would be advantageous. However, the imprint retention was not as robust in those early days. We didn't appreciate the importance of conditioning the local environment for this class of experiment, and we introduced the variable of uncontrolled physical convection into the protocol. With the passage of time and repeated experiments, we sorted out the various factors involved and conducted the experiments in a single location with simultaneous water exposure to a device and pH measurement. With time, the experiments moved away from the use of Evian water because of the variable and thus uncontrollable degree of Ca/Mg carbonate precipitation involved. Later experiments with $ZnCO_3$ crystallites did not suffer from this problem because $ZnCO_3$ is only very sparingly soluble in water.

B. Fruit Fly Target Experiment: This study involved ~ 10,000 larvae and 7,000 adult flies assessed over an 8-month period [5]. Larval development time, $t_{1/2}$, the time taken for half the surviving adults to emerge, was measured at 18 °C and 55% RH. There were three experimental variants with respect to the control culture (C) placed on a typical lab bench top. These were, (F) an identical culture in a Faraday cage with no device present, (d,o), an identical culture in a Faraday cage with an active unimprinted device present and (d,j), an identical culture in a Faraday cage with an active imprinted device present. All treatments

were placed next to each other on a laboratory bench at 18 °C and the experiments conducted simultaneously.

The particular device was placed in the center of a Faraday cage with vials placed around the perimeter ~ 15 cm away (see figure 3). At the end of a specific time interval, the device was turned off and removed from this cage. The larval development continued. A single replicate involved 30 larvae (0-4 hr. old) transferred to a vial containing non-stressful food. The vials were monitored daily and surviving adults collected. There was a minimum of 15 replicates (vials) per treatment.

The [ATP]/[ADP] ratio for these flies was measured in the presence of (1) supplemental pure H_20 or (2) supplemental 0.01M NAD. The ATP, ADP and AMP were extracted using 4.2M formic acid and 4.2M ammonium hydroxide. Quantification was made via an automated Isco HPLC unit, a VYDAC column and a pre-programmed gradient from 0.025M to 0.5M sodium phosphate monobasic (pH = 2.8). There were 8 replicates per treatment for both supplemental NAD and pure H_20.

C. Enzyme Target Experiment: Once again, as in B, three comparison treatments occurred, (C) with (F), (d,o) and (d,j) [7]. The local enzyme-vessel arrangement is shown in figure 4. The protocol utilized was to expose the water and quartz tubes without the enzyme to the four treatments for a period of 2 days. Next, with the ALP solution present, all treatments were exposed for 30 minutes. Three dilutions of the ALP, 100 µl ALP solution plus 150 µl pure H_20, 200 µl pure H_20 and 250 µl pure H_20, were studied. After this, the ALP activity was measured.

The enzyme activity was measured using the VITROS DT60 chemistry system with the DT6011 analyzer and DTSC 11 module from Johnson & Johnson Clinical Diagnostics Inc. This system gives results in 2-5 min. The VITROS DT controls are available as vials of

frozen lyophilate and serum. Enzymes are present in the lyophilate with the ALP being derived from porcine kidney.

The VITROS ALP-DT slide is a dry multilayered film in a plastic support. In 10 µl of serum or plasma, it contains all the reagents needed to determine thermodynamic activity. The primary reaction is based on ALP catalyzing the hydrolysis of p-nitrophenyl phosphate to p-nitrophenol. The p-nitrophenol then diffuses to an underlying layer where its concentration is monitored by reflective spectroscopy.

Experimental Results

A. Water Target Experiment: Early experiments at Stanford with Evian water and pH-lowering devices showed us three things, (1) an intention-induced pH effect was present (see figure 5) although not nearly as large as intended because of unanticipated Ca/Mg carbonate precipitation, (2) one could see a time-dependent growth and decay of a unique pH-signature that appeared to be related to both gradual local environment conditioning and gradual leakage of the "imprint-charge" from the IIED over a two-month period (see figure 6) and (3) a clearly distinguishable difference was apparent in the coherence in the pH-data between the water treated with an active unimprinted device (relatively incoherent) and an active imprinted device (much more coherent). This difference is illustrated in figure 7 with the day-by-day pH-plots after exposure of the water to these devices.

The 50/50 Castle Rock water plus ASTM Type I purified water experiments, initially conducted at Stanford and continued in Minnesota with pH-lowering devices, eliminated the uncontrolled Ca/Mg carbonate precipitation and allowed large, robust pH changes to be recorded. This is illustrated in figure 8 for the two cases, (a) simultaneous water exposure to an active IIED and pH measurement over a 5-day period and (b) a preliminary 5-day

exposure to the active IIED without pH measurement, removal of the active IIED to its Faraday cage and then continuous pH measurement of this pretreated water. The similarity of the two curves seems remarkable.

To prove that IIED's are not limited to pH-lowering effects, IIED's with pH-raising intention were next prepared in California and shipped to the Minnesota lab for testing with 100% Type I purified water. Figure 9 shows the very first piece of experimental data obtained with these newly prepared devices. It was most satisfying to see that a ΔpH of one full pH unit had been achieved. Comparable data of this nature was observed over the next 3-4 months as the imprint charge slowly leaked from the devices.

To further test the idea suggested from previous work that the imprinted water (after treatment by an active IIED) might transfer an imprint-effect to crystals grown from that water which, in-turn, might transfer the imprint-effect to fresh water, we utilized some of the Ca/Mg carbonate crystals from the Evian water studies. These crystals were carefully washed and then added to a vessel of new, untreated water. The crystals dissolved in this water and transferred the imprint-effect to this fresh water. However, even though a transfer-effect had been observed, was it due to partitioning of the original imprint to these crystals as they grew from the imprinted solution or was it merely due to entrainment of some of the original water at defect surfaces in these crystals formed as a consequence of their uncontrolled mode of growth? Further, because of unanticipated metastable phase formation from uncontrolled solution supersaturation and precipitation, even if real imprint partitioning had occurred, we didn't know which crystalline phase was the culprit. To correct this deficiency, we set about to carefully grow specific crystals under well-defined conditions so as to test this partitioning hypothesis. The sparingly soluble material, $ZnCO_3$, was chosen as the first test material and, during the course of that investigation, a phenomenon arose that sent the experimentation down a different path. Thus, the crystal-partitioning

study is unfinished but this new phenomenon, to be described below, has been diligently pursued.

As a consequence of the $ZnCO_3$ crystal growth experiments, we began to add fine particles of commercially available, sparingly soluble $ZnCO_3$ to purified water and performed a variety of experiments with a solution containing 4 g/l of fine $ZnCO_3$ particles (having a surface area of 21.4 m^2/gm). Although the new phenomenon could sometimes be obtained with no $ZnCO_3$ particles present, it was almost a constant phenomenon when the $ZnCO_3$ particles were present in the water. This new phenomenon was the appearance of both low frequency and appreciably higher frequency oscillations in the pH-time curves (see figure10) [6]. Such oscillations in pH should not be possible according to the second law of thermodynamics in systems close to or at equilibrium.

The results of figure 10 were generated via a particular two-vessel experiment. Vessel A contained a solution of ASTM Type I pure water plus 4 g/l $ZnCO_3$ particles with an IIED about one foot away. Vessel B was ~ 150 ft. away in another building, contained the identical type of solution with solid particles and was simultaneously pH-monitored and temperature-monitored but had no IIED nearby. As can be seen from figure 10, at location B, the long-period oscillations, τ_L, exhibited $\tau \geq 20$ hours while the short-period oscillations, τ_S, are reduced by a factor > 10. A particularly interesting highly periodic short-period oscillation train with diurnal repetition can be observed between 65 and 108 hours in figure 10. The damped followed by undamped series of oscillations repeats on two consecutive days.

In further experiments, a new transmitting station (location C) was established about 115 feet from location B in another building. Similar to the A-B transmission series, a pH-lowering device was placed at location C about one foot from a vessel containing pure water with $ZnCO_3$ particles as above. There was no IIED present at location B following the

previously established protocol. The inset in figure 11a is a magnification of a portion of the τ_S-oscillation profile from this C-B transmission experiment [6] while figure 11b is a further magnification to illustrate the highly periodic nature of these oscillations. Figure 11a gives the Fourier amplitude spectrum for the data shown in the inset. Here, one can note an exponential-like intensity decay with increasing frequency wherein the fundamental period is $\tau_S \sim 64$ min.

Although the τ_L-oscillations appear to be connected to either diurnal, solar or lunar rhythms, the τ_S-oscillations appear to be connected to the activation (on) vs. deactivation (off) of the IIED. The results shown in figure 12 are from simultaneous pH measurements in two vessels , B and C, with exposure of vessel C to an imprinted pH-lowering device 115 feet from B. Both vessels contain pure water with $ZnCO_3$ particles as above. In figure 12 (a and b), by comparing the pH-time curves for locations B and C, one notes that a kind of "beating" correlation exists between the two systems wherein B appears to periodically move in and out of relative phase coherence with C.

Another interesting observation is presented in figure 13. Here, we see in another experiment, the pH-time curves for locations B and C with a small amount of correlation between them but, because the IIED close to C has been turned on, one expects the plot for B to be generally decreasing and it is not. However, by shaking vessel C, an abrupt and substantial decrease in $(pH)_C$ occurs with accompanying large amplitude τ_S-oscillations over subsequent days while nothing particularly significant happens to $(pH)_B$. The shaking of vessel B ~ 24 hours later produced an abrupt decrease in $(pH)_B$ even though no active IIED was close to B. Again, as in $(pH)_C$, the τ_S-oscillation amplitude increased in vessel B after its shaking event.

In figures 14a and b, one sees simultaneous pH and temperature measurements in vessel B with exposure of a similar vessel to an imprinted pH-lowering device at location C

115 feet away in a different building. Again, as before, the two vessels contain 1 g $ZnCO_3$ particles in 250 ml pure water. Without the IIED being turned on at location C, the temperature profile at B does not have the pronounced flat periods near temperature minima. Of course, it is well known that there exists a conventional mathematical relationship connecting temperature and pH – but this is not it! Here, after the IIED has been turned on at location C as indicated in figure 14a, the pH changes in the direction of its prime directive with significant amplitude τ_S-oscillations at location B. Looking carefully at figure 14a, one notes that the bursts of pH-oscillations correspond with the nearly periodic shallow minima present in the temperature profile. Somehow, these T-undulations and pH-oscillations are connected, but not in the conventional way. Figure 14b is a closer view of this type of coupling.

Perhaps the most important observation of this study made to date is that continued use of the IIED's at a particular locale conditions that locale in such a way that oscillations in various properties of water (pH, temperature, conductivity) occur without the further use of an IIED. This was first noticed via a strong correlation between the τ_S-oscillations in vessels B and C when locale B was one that had been utilized a great deal during these experiments. However, when vessel B was moved to a new location, several hundred feet from C, no pH-oscillations were initially obtained (neither τ_L nor τ_S); but, with continued use at that new location, the oscillations slowly grew. Once the environment has been conditioned in this way, oscillations in water properties can be studied without the use of IIED's. Figures 15a and b illustrate some of the in-phase oscillations in water properties that occur in various aqueous solutions exposed only to a conditioned environment.

B. Fruit Fly Target Experiment: The experiments presented here deal with an environmental treatment effect; thus, we adopted a conservative statistical approach and

treated the population means for the four experiments as the primary data. The ANOVA is given in Table 1 and it indicated a significant treatment effect for larval development time, $T_{1/2}$, with the following treatment rankings: $F < C \leq d,j \leq d,o$. Figure 16a gives the mean values for the fitness components and treatments, calculated using the mean values from the four experiments. Considering the results for the two categories of devices assessed, a pairwise comparison of d,j vs. d,o was significant as follows: $t_3 = 10.753$ ($p = 0.002$). Additionally, a pairwise comparison of C vs. F gave $t_3 = 3.813$ ($p = 0.03$).

Results for the [ATP]/[ADP] ratio in the presence of both NAD and pure H_20 indicated statistical significance as follows: $F > C > d,j > d,o$ (see figure 16b and Table 1). Considering results for the two different categories of devices, d,j and d,o, pairwise comparisons were significant as follows: NAD gave $t_7 = 6.497$ ($p < 0.001$) while pure H_20 gave $t_7 = 3.091$ ($p = 0.02$), a much less significant result.

C. Enzyme Target Experiment: Here, comparisons are made between the control ALP solution on a shelf in an incubator at 4 °C with (1) an identical ALP solution in a small Faraday cage (F) which is located adjacent to C on the shelf and no device is present, (2) the same as (1) but with an imprinted device present (d,j) and (3) the same as (1) but with an unimprinted device present (d,o). All four experimental states (C,F,d,j, d,o) were located next to each other on the shelf. A core experimental system comprising 100 ml quartz tubes placed in beakers containing 100 ml pure H_20 was utilized. This system, without the ALP solution was first exposed to the particular treatment (C,F,d,j, d,o) for 2 days. Then fresh enzyme solution was prepared and transferred to the quartz tubes followed by 40 minutes of exposure to the particular treatment (see figures 4 & 17). At the end of this period, ALP activity was determined as the mean of 7 replicate assays for each treatment.

ALP activity was measured with the VITROS DT60 chemistry system, the DT6011 analyzer and the DTSC11 module (Johnson & Johnson Clinical Diagnostics, Inc.). VITROS

DT control enzyme solutions were used as experimental material. The ALP was derived from porcine kidney and standard procedures were followed. The VITROS ALP DT slide is a dry, multilayered film in a plastic support. It contains all the necessary reagents to determine activity in 10 $\mu\ell$ serum or plasma. The reaction is based on ALP catalyzing the hydrolysis of p-nitrophenyl to p-nitrophenol. The p-nitrophenol then diffuses into the underlying layer where its concentration is monitored by reflectance spectrophotometry. The process starts by depositing a 10 $\mu\ell$ drop of solution on the slide which is evenly distributed by the spreading layer. The experimental means and standard deviations for ALP activity are given in figure 17 and show the relationship (d,j) > F > C > (d,o) for both dilutions ($p < 0.001$). Considering the results for the two categories of devices assessed, a pairwise comparison of d,j vs. d,o was significant as follows: $t_{13} = 4.007$ ($p = 0.001$). Additionally, a pairwise comparison of C vs. F gave $t_{13} = 2.871$ ($p = 0.01$).

A Relevant Theoretical Perspective

In expert systems and intelligent machines, hardware architecture with supportive written software allows the machines to perform within precise, predictable limits. Some variations in the preciseness of these limits can be expected if "fuzzy logic" is involved via the software. However, in relatively simple electronic systems, one has come to expect that the output performance can be completely and exactly characterized based upon the system design along with its specific material and electrical component parameters; i.e., the output response / input signal ratio is independent of any other factors than these. Certainly, the great success of computer-aided design (CAD) for both electric circuit design and semiconductor processing procedures utilized for integrated circuit fabrication underscores the utility of this paradigm in today's technology.

In quantum mechanics (QM), philosophical attention has been given to the possibility of consciousness affecting the collapse of the wave function; however, nothing specific and detailed has been developed to show how consciousness might alter the "numbers" in a practical application wherein consciousness is of significant importance. One of the difficulties here is that consciousness cannot yet be quantitatively expressed in terms of the potentials that enter Schrödinger's equation for the wave function. Another is that this wave function is limited to expression in our conventional four-space of distance-time. Thus, although QM supposedly deals with "all that is", the mathematical formalism is sufficiently complex that one does not obtain much insightful illumination from carrying out QM calculations.

One possible reason for the lack of physical insight arising out of QM calculations is because the base-space used in QM for viewing nature is our familiar (x,y,z,t)-space. With this choice, we are required to attribute wave-particle duality characteristics, non-local force characteristics, magnetic dipole characteristics, etc., to particles of matter. Instead of continuing along this familiar path, suppose we define a more appropriate base-space for viewing nature, one which quite naturally expresses both wave and particle behavior, non-local forces, electric and magnetic monopoles and allows both human consciousness and human intention to influence physical reality. The purpose of this section is to lay out such a model previously proposed by one of us [2].

In a recent book [2], Tiller has given a fundamental account of his multidimensional model of nature as a basis for explaining subtle energy phenomena. In turn, subtle energies have been defined as all those other than gravity, electromagnetism, the weak nuclear force energies and the strong nuclear force energies. Subtle energies are, in fact, vacuum energies. This model is most simply illustrated by figure 18 wherein our familiar 4-space has a dual 4-space partner to comprise a unique 8-space. The dual 4-spaces are (a)

our familiar direct 4-space (D-space) and (b) its reciprocal 4-space (R-space). This 8-space is imbedded in a 9-space (the emotion domain) which, in turn, is imbedded in a 10-space (the mind domain). The embedding frame for all of this is the domain of spirit (11-space).

Since the natural co-ordinates for D-space are (x,y,z,t) and for R-space are $(x,^{-1},y,^{-1},z^{-1},t^{-1})$, this dual pair of 4-spaces provide, quite naturally both particle and wave expressions for substance. The electric monopole part of this substance responds to fields present in D-space, have positive energies, positive mass and obey the laws of relativity theory. The magnetic monopole part of this substance is proposed to respond to fields present in R-space having negative energies (and is thus the first layer of substructure in the vacuum), negative real mass and are superluminal. It is this R-space magnetic substance that is thought to write the de Broglie pilotwave envelope that is conjugate to the D-space electric particles [3]. Normally weak coupling is thought to exist via a substance of the 9-space emotion domain, called deltrons, which can resonate with both electric and magnetic substance without concern for relativistic singularities. However, strong coupling is possible when intention from 11-space creates a mind domain imprint that, in turn, increases the deltron activity [2].

A special inversion mirror type of relationship is proposed to operate between the dual 4-spaces so that monopoles in the one 4-space create image dipoles in the companion 4-space. This leads to our usual Maxwell equations in D-space and another set of Maxwell-like equations in R-space. Because of the Fourier Transform relationship acting between these two 4-spaces, it has been shown that the undulation intervals of the helical R-space waves control the position, velocity, acceleration and locus of the particle-like moieties in the "now" of D-space [3].

In the early part of this century, x-ray crystallographers developed the concept of the reciprocal lattice and the importance of the Fourier Transform (FT) to the process of

diffraction became appreciated. This eventually led to the generalized concept of reciprocal space wherein the phase variation along a line in R-space normal to a plane in D-space is controlled by the distance, **s**, of the plane from its origin [10]. The value of the reciprocal at a point with distance **k** along the normal to the plane of weighting ω is just $\omega \, exp\,(2\pi\, i\ s\bullet k)$. Thus, defining ρ_S as the density of a particular quality in a D-space object (mass, charge, potential, ternperature, etc.), the equilibrium conjugate quality in R-space is given by the FT, F(k), and vise versa. The transformation from D-space to R-space, T, and the reverse transformation, T^{-1}, for one-dimension, are given by

$$T: \qquad F(k) = \frac{1}{\sqrt{2\pi}} \int_{D-space} \rho_s \, e^{\,i2\pi\, s\bullet k}\, ds \quad , \qquad (1a)$$

$$T^{-1}: \qquad \rho_s(s) = \frac{1}{\sqrt{2\pi}} \int_{R-space} F(k)\ e^{\,-i2\pi\, s\bullet k}\, dk \quad . \qquad (1b)$$

As is well known, D-space to R-space transformations of any number of dimensions can be treated in this way [11,12].

One of the most intriguing features associated with broadening our perspective on the use of these Fourier mates expressed by Eqs. 1 is that they implicitly embody wave and particle expressions of a particular quality of substance that one can discriminate for our D-space object. Thus, one of the cornerstones of QM is implicitly built into physics when one attends to both D-space and R-space counterparts of an object. Interestingly, non-local effects are also naturally built in because the quality density in a particular small region of D-space is given in terms of an integral over the entire domain of R-space and thus separated

D-space regions are connected to each other via the total R-space domain. For an object located at x = 0 in D-space, let its R-space equilibrium counterpart be F(k). Then, if the object is moved to x = Δx, its R-space equilibrium counterpart is given by $e^{i2\pi \Delta \mathbf{x} \bullet \mathbf{k}}$ F(k). We see that this counterpart maintains the same k-dependence except for a phase factor that grows with $\Delta \mathbf{x} \bullet \mathbf{k}$ so the effect is the same oscillating function with k no matter how large Δx becomes.

The magnetic monopole/magnetic dipole image feature introduced here creates no operational problems for D-space magnetism or electromagnetism. It merely requires a reinterpretation of the magnetic quantum number for atoms [3].

How the nested dimensional frames of figure18 are proposed to synergistically work together to transfer intention from the domain of spirit to the domain of our D-space cognitive awareness is given in figure 19. The intention is first imprinted onto the 10-dimensional nodal network of the mind domain [2]. This primary imprint is transferred via a diffraction-type process to yield both a secondary imprint on the nodal network of R-space and an activation of the special emotion domain substance called deltrons. The deltrons allow coupling between the R-space imprint and the nodal network of D-space, also via a diffraction process. It is this D-space imprint that sets in motion all forms of action in the physical domain [2]. These three nodal networks give a structure to space that has not yet been revealed by present-day science. At present, most scientists think of space as a continuum.

The foregoing model requires a base-space of at least 9-dimensions with dual reciprocal 4-spaces in order to account properly for normal electromagnetism (with no human interaction). In this case, any higher dimensional inputs are treated as boundary conditions on the R-space nodal network. To treat human psychoenergetic phenomena, the model requires a base-space of at least 10-Dimensions with higher dimensional inputs

treated as boundary conditions on the mind domain nodal network. In this model, consciousness relates to the unknown wave substance that diffracts through these three nodal networks [2].

Discussion

It seems clear from the experimental data that, at least here, intentionality has been elevated to the status of an important variable influencing the key physical processes in these target experiments. How are we to understand this when there is such a large body of data that supports the opposing position? To proceed, let us first see where in today's description of physics do we see allowable possibilities for "windows" through which subtle domain forces could act and how these possibilities might lead to an IIED. Next, let us see how such devices, via an on/off switch appear to be able to broadcast a "prime directive" to the different target experiments. Next, what aspect of this "broadcast" might activate the key physical processes needed to yield such target experiment results? Finally, what is so special about these acts of intention embodied by the IIED's that they have generated such robust results when so many other approaches have not?

Two Allowable Windows: In the 1920's, Dirac utilized relativistic quantum mechanics to evaluate the interaction between a physical electron and the vacuum [13,14]. His equations predicted not only positive energy states but negative energy state solutions. From this, he postulated that the vacuum consisted of all these negative energy states and they were all filled. Nevertheless, by stimulating this negative energy state distribution via a photon with sufficient energy, a particle (electron, say) may be promoted into one of the allowed positive energy states and become physically real (i.e., observable). The hole left behind in the negative energy spectrum is the antiparticle (positron in this case). To date, antiparticles

have been found experimentally for all the particles known to physics. Today, the vacuum is seen as a chaotic sea of boundless energy (energy density equivalent to ~ 10^{94} grams per cc) with incredibly large destructive interference of virtual particle wave functions.

It is the QM interactions between this virtual particle sea and the electron that constitute the ground state energy, μ_o^e (e = electron), at conditions of standard temperature and pressure. This same approach applies for all elementary particles which then may combine to form atoms and molecules. So the bottom line is that the standard state thermodynamic potential, μ_o^j, for any species, j, involves the interaction of j with the non-physical stuff that constitutes the negative energy sea of the vacuum. In terms of the discussion of the previous section this largely means the interaction between a D-space particle and its R-space counterpart (first structural layer of the vacuum).

A few years ago, one of us proposed that if, from a deep meditative state, focussed human intention could shift the degree of coherence in the virtual particle sea of the vacuum by even a tiny amount, the ground state energy of the electron, other elementary particles, atoms and molecules should be appreciably altered [1]. From this basis, one might expect that μ_o could be altered by focussed human intention so it is necessary to include the following equation:

$$\mu^j_{0A} = \mu^j_{\infty A} + \Delta\mu^j_{0A} \quad . \quad (2)$$

In (2), A is the medium, μ_∞ is the baseline standard state chemical potential in the absence of directed human intention and $\Delta\mu_o$ is the contribution to be associated with directed human intention. It should also be recognized that evolutionary changes in collective human consciousness might cause a drift in $\mu^j_{\infty A}$. It has also been postulated that focussed

human intention from subtle domains produces a change in magnetic vector potential, $\Delta\bar{A}$, in our physical domain which, by our standard equations of electrodynamics, produces changes $\Delta\bar{E}$ and $\Delta\bar{H}$ in our ambient electric and magnetic fields [15]. Such changes in $\Delta\bar{E}$ are likely to change the ambient electrostatic potential, V, from the baseline macropotential, V_o, in the absence of focussed intention so we also define

$$V = V_o + \Delta V \quad , \qquad (3)$$

where the contribution ΔV is attributed to the effect of directed intention. Combining the standard thermodynamic formula for chemical potential with Eqs. 2 and 3 into the effective chemical activity, a', format, we obtain for the generalized potential, η_A^j ,

$$\eta_A^j = \mu_{\infty A}^j + kT \ln(a'^j_A) + z^j e V_o \qquad (4a)$$

with

$$\frac{a'^j_A}{a^j_A} = \exp\left\{\frac{\Delta\mu^j_{0A} + z^j e\,\Delta V + \frac{1}{2}\left[\varepsilon_A(\bar{E}+\Delta\bar{E})^2 + m_A(\bar{H}+\Delta\bar{H})^2\right]}{kT}\right\}. \qquad (4b)$$

Here, T = temperature, k = Boltzmann's constant, a = chemical activity ($a = \gamma c$ where c = concentration and γ = activity coefficient), e = electron charge, z = valence, V = electrostatic potential, ε = electrical permittivity, m = magnetic permeability, $\bar{E}$ = electrical field and $\bar{H}$ = magnetic field. Clearly, from Eq. 4, both electromagnetic fields and intention-generated potential effects can influence thermodynamic and kinetic-limited processes in both organic

and inorganic materials. Certainly standard EM effects are seen in the fruit fly studies when comparing treatments C and F. Likewise, robust subtle domain effects are seen in all three target experiments.

Broadcasting a Prime Directive:

From the experimental results, one can conclude that the IIED's have, at least under these circumstances, a real effect on physical materials, inorganic and organic. The simplest postulate would seem to be that such effects are somehow related to the EM waves emitted by the oscillators in the devices. These EM waves are actually photons, albeit photons with very long wavelengths and quite low energy, and, as such, each has a de Broglie pilot wave built from R-space components. Our postulate is that, it is not the D-space interaction between the photons and the water, fruit fly larvae or ALP that produces these unexpected results but, rather, it is the R-space counterparts of the photons that are interacting with the R-space counterparts of the water, larvae or ALP to drive these changes. From the theoretical model, the Maxwell equations in D-space couple to an analogous set of equations in R-space via deltron activation [2,3]. The mathematically real part of this interaction, at very low deltron activation, is what we call electromagnetism. At significant deltron activation, new terms are thought to enter this non-linear coupling interaction, and it is these terms that lead to the present experimental results in D-space. The addition of the mathematically real part of these non-linear interactions to the conventional linear interactions, we call "augmented electromagnetism". We will hereafter use the rubric "intention-augmented EMF's" to indicate that some new type of association with EM-waves has occurred which allows a specific intention to interact with the target.

From a thermodynamic perspective, consider Gibb's phase rule[16] which tells us, for equilibrium conditions, the number of degrees of freedom, f, available to a system of C components when there are p coexisting phases present. For the usual physical reality case with only two extrinsic variables, temperature, T, and pressure, P, the phase rule statement is

$$f = C - p + 2 \ . \qquad (5a)$$

Thus, if we have only one component (C = 1) and one phase present (p = 1), T and P can be varied independently (f = 2) without changing the phase so this is called a bivariant domain. When there are two coexisting phases (p = 2), it is a univariant condition (f = 1) that obtains and there is some constraint relationship operating between T and P (one is fixed by the other). When there are three different material phases present (p = 3), it is an invariant condition (f = o) that obtains and equilibrium can occur only at a single point in the entire (T, P) variable space. At all other points in this variable space, thermodynamics requires material phase transformations to be occurring.

The present experiments tell us that, at least under some conditions, intentionality, I*, and probably consciousness, C*, are also thermodynamic variables for D-space. Thus, in Gibb's phase rule, we must increase our number of <u>independent</u> thermodynamic variables by two (I* and C*). So that the phase rule statement now becomes

$$f = C - p + 4 \qquad (5b)$$

and many more degrees of freedom are available for equilibria to occur between multicomponent/multidimensional phases in nature. Now, instead of the expected invariant or univariant condition in (T, P) variable space, one can achieve bivariant or trivariant

equilibrium (stable) conditions in D-space at the same T and P because of the unseen and unappreciated additional variables I* and C*. Because of this, it is not surprising that new stable phenomena can appear.

D-Space Process Activation: A specific intention to be fulfilled in D-space requires a certain set of processes in D-space to operate in a particular way. This, in turn, requires that a certain thermodynamic potential map be applied to D-space with the rate of fulfillment of the intention in D-space being determined by the D-space kinetics involved. As an illustrative example, the D-space transport flux, F_A^j, of the j species in medium A is given in terms of its mobility, M_A^j, by

$$F_A^j = M_A^j \nabla \eta_A^j \ , \qquad (6)$$

where $M_A^j = D_A^j C_A^j / kT$, D is the diffusion coefficient and η_A^j is the electrochemical potential given by Eq. 4a. Thus, one sees how EM and subtle domain effects enter this aspect of the kinetics (via Eqs. 4).

If one defines this required thermodynamic potential map, mentioned above, in terms of certain geometrical fields and potentials in D-space, the equilibrium R-space counterparts of these are given by various Fourier Transforms (FT's). It is proposed that there is a lawful way whereby the higher dimensional intention can be first expressed in R-space by these specific FT's so that the inverse FT's then act as forces on D-space to cause these desired manifestations to eventually appear in D-space. If we take the example of pH-change in water as our target, then some of the D-space processes that might be involved would be (1) the dissociation reaction of H_20, (2) the solubility reactions of CO_2 and O_2 in water and (3) any acid or base dissociation reaction for dopant species present in water. Alterations at

the vacuum level probably change the equilibrium constants for these chemical reactions sufficiently to bring about the desired changes.

What Is So Special Here?: It is well known that most individual humans have intentions that swing widely over time so that the time-averaged effect over weeks to months is usually of small magnitude. Individual humans having long practice with one of the available inner self-management techniques like Yoga, QiGong, Sufism, HeartMath, etc., do much better but there is still some time-averaging limitation involved. Precipitating a specific intention into a device during a 1-2 hour session eliminates much of this swing.

Group intentional efforts in this direction, especially those focussed on healing prayer, have been successful both locally and non-locally [17,18]. From studies in the area of healers, one generally finds that those who are most effective exhibit not only significant inner self-management and physiological coherence of their bodies, but they acknowledge that it is "unseen" forces of the Universe that do the healing work through them. They generally think of themselves as a participating conduit for the passage of these energies/information into and through R-space/D-space. Such a communication system for information and power transmission involves both the effective band width and signal/noise ratio with respect to the specific held-intention and the power handling capacity of the channel at R-space/D-space levels [2].

It is also well known that the effective output of cooperative group efforts depends upon both the number of units contributing to the group and the degree of internal coherence of the group. For such a case, the best possible result is given by $(N\overline{A})^2$, where N is the number of units cooperating in the group with average output amplitude for each unit of $\overline{A}$ [2]. When one begins to discriminate the "seen" D-space group from the "unseen" subtle domains group, the picture obviously becomes much more complex. However, one

can begin to see that the effective N in this simple formula might be very large. This could allow the collective field impressed on the electronic device to move strongly into the non-linear domain of D-space/R-space physics. Utilizing an electronic device to somehow store this collective, specific intent in some presently undefined structural phase of the vacuum has many obvious advantages.

There also appears to be an adaptation of the local environment to the use of these IIEDs so that the local environment becomes more responsive to the broadcast prime directive, almost as if there were a D-space "readiness" for this evolutionary step in collective human consciousness. Since things are first manifest in R-space prior to their "playing out in time" at the D-space level, the IIEDs may serve also as a kinetic mechanism whereby the higher potentialized thermodynamics can be unfolded.

Device Isolation Considerations: Early on in this experimental program, it was discovered that, even in the electrically switched-off state, some form of information leakage was occurring between the imprinted device and the unimprinted control device. This manifested as a temporally decreasing difference in the results found when the devices were separately used in the target experiment. The present solution to this difficulty was to store each device in its own electrically grounded Faraday cage after first completely wrapping it in aluminum foil. The theoretical rationale used here was that subtle domain substance interacts with D-space substance via a process that manifests a magnetic vector potential contribution, $\Delta\overline{A}$, at the D-space/R-space interface. This is thought to be a type of equilibrium partitioning. Since it is well known from standard electrodynamics that $\Delta\overline{A}$ can produce an electric field effect, $\Delta\overline{E}$, and a magnetic field effect, $\Delta\overline{H}$, [19,20] then augmented-EM radiation between the devices (even in the off-state due to fluctuating environmental EMFS) and the environment might allow information transfer. This, in turn, would tend to

reduce $\Delta\overline{A}$ which would, in turn, dissipate the intention charge in the subtle domain. In any event, although not perfect, this procedure has allowed the intention charge to be stored in the devices for ~ 3-4 months and significantly diminished the apparent communication between the imprinted and unimprinted devices.

Conditioning, Coherence and Oscillations: Experimentally, the data shows that continued use of an IIED leads to stronger and stronger correlations between simultaneously measured pH-oscillations at two or more remotely located vessels of water plus $ZnCO_3$ particles. The particular remote locales seem to be growing in structural coherence with respect to the transmitter vessel locale. In the framework of the theoretical multidimensional model of the previous section, this possibility is associated with the nodal network (NN) ordering in both R-space and D-space [(2)]. With respect to this model, it must always be remembered that events occurring in R-space are precursors to correlated events appearing in D-space at some later time. If the event imprint manifests in the high frequency region of the inverse time coordinate of R-space, then it materializes in ~ "the now" of D-space. If the event imprint manifests in the low frequency region of the t^{-1} coordinate of R-space, then it materializes in what we call " the future" for D-space. It is the inverse Fourier Transform relationship that yields the particular Δt needed from the "now" before materialization is possible in D-space [(2,3)].

A brief outline of the proposed picture operating here is that (1) the mind NN is fully ordered, (2) the specific intention strength increases and the focus sharpens, largely due to inputs from cooperative unseen forces, (3) the diffracted beams from the mind NN are sufficiently strong to stimulate NN self-entrainment towards enhanced order at the R-space level (something like pumping a laser crystal towards the lasing threshold), (4) the intention imprint occurs at several different octaves of R-space (multiple orders of diffraction) and (5)

with sufficient R-space/D-space coupling, a D-space NN ordering reaction can also occur which, in turn, modulates the materialization of new D-space phenomena [2]. The greater is the initial degree of NN disorder at the D-space level, the greater must be the degree of R-space to D-space pumping needed for D-space NN self-entrainment to an ordered state. The τ_S, pH-oscillations observed in D-space are thought to reflect fluctuating states of R-space NN order & consequently D-space NN order oscillations in time (and space).

Necessary & Sufficient Conditions For Repeatability: Imbedding subtle energies into a device and then using the device in a particular experiment tends to partially "objectify" the subtle energy. If the subtle intention-charge can be retained in the device for some months, then this would allow many different laboratories to perform the same experiment with either the same devices or with similarly processed devices. This would tend to more fully objectify the subtle domain imprint influencing the course of D-space reality.

From the authors' present perspective, the following is a list of the discriminated factors influencing these experimental results: (1) The imprinter's training, degree of inner self-management and internal coherence, heart focus and intentions, (2) the details of the imprinting procedures, (3) the unseen network of forces cooperating with the imprinters, (4) the D-space design, components and materials of the device, (5) the isolation efficiency between the physically identical unirnprinted and imprinted devices (this includes shipping), (6) the particular D-space locale used for the experiments (affects the amount of conditioning needed), (7) the degree of inner self-management of the actual experimenters, (8) the held attitudes of heart and mind of the experimenters during the course of the experiments and (9) the number of times the experiment is repeated in the particular locale.

In the beginning, it would probably be most efficient to utilize the same imprinters and devices for any replication attempts. However, after some continued experience with this mode of operation, it would be useful to explore other possibilities. We are at present exploring the length of conditioning time a new locale needs with a space conditioning device in order to move from the weak coupling condition to the strong coupling condition in that new locale.

Philosophical Significance For Humanity: From this work, it seems clear that human consciousness can influence physical reality via a time-averaged specific intention. One can deduce from this that D-space reality is not the primary reality but seems to be the consequence of collective human intention impressing patterns on more subtle domains of the universe. Thus, one's thoughts and attitudes held during common daily D-space actions appear to participate in reprogramming humanity's collective D-space future. Recognizing this as a sequence of creation events, one can readily see that adopting the discipline of inner self-management and self-directed coherence development at all levels leads to more effective creations.

One can also see that D-space is adaptable and that IIED's can help to clean up old technology mistakes, enhance the efficiencies of present D-space technologies and create a large variety of new ones. Clearly, this will involve a shift to a new physics paradigm for nature and our relationship to it. Further, by expanding one's mindset to embrace this unfolding picture, people are expected to begin to develop cognitive awareness of patterns of information in R-space.

Pribram [21] has written extensively on the brain processes involved in visual imaging. From his viewpoint, a D-space information pattern enters the body via the circular lens of the eye and, eventually, it activates the input and operator neurons of the brain's cortical

columns. This leads to overlapping receptive fields of interneurons, which are tunable by adaptation and habituation. Each interneuron thus acts like a bin in a computer that stores the averages of the part of the pattern to which it has been exposed. The ensemble of receptive fields (bins) stores the average pattern. When one plots these receptive field patterns, they bear a marked correlation to the Gabor Function (like a Hartley Function, the Gabor Function is a FT over a finite domain rather than over the infinite domain) of the D-space pattern impinging on the iris of the eye [(2)].

A general view of this, then, is that cortical neurons act like individual receiving antennas in a large array converting D-space information into a diffraction pattern whose mathematical representation is very close to the particular FT. This information conversion to the particular frequency domain appears to be ideal for subsequent brain processing and brain perception. Conscious awareness of the outer world (D-space) information also requires the occurrence of an inverse FT in the later stages of the processing chain. For our purposes here, this indicates that both R-space and D-space information maps of the primary input information are available at some unique locations of our brains which suggests that it may indeed be possible for humans to have cognitive awareness of the R-space band in the overall spectrum of reality.

One last philosophical consideration for humanity that may arise out of this work is the realization of, and the acceptance of, the fact that there are many potentially cognitive bands in the overall spectrum of reality!

Acknowledgements

This work was partially supported by Ditron, LLC.

References

[1] W.A. Tiller, What Are Subtle Energies?, J. Sci. Expl. 7 (1993) 293.

[2] W.A. Tiller, "Science and Human Transformation: Subtle Energies, Intentionality and Consciousness", (Pavior Publishing, Walnut Creek, CA, 1997).

[3] W.A. Tiller, Towards a Predictive Model of Subtle Domain Connection to the Physical Domain Aspect of Reality: Origins of Wave-Particle Duality, Electric-Magnetic Monopoles and the Mirror Principle, J. Sci. Expl. 13, 1 (1999) 41.

[4] W.E. Dibble, Jr. and W.A. Tiller, Electronic Device-Mediated pH Changes in Water, J. Sci. Expl. 13, 2 (1999)

[5] M.J. Kohane and W.A. Tiller, Energy, Fitness and Electromagnetic Fields in Drosophila Melanogaster, submitted to J. Sci. Expl.

[6] W.E. Dibble, Jr. and W.A. Tiller, On Augmented Electromagnetic Wave Communication between Remote Vessels of Water Containing $ZnCO_3$ Crystallites. I. Initial Two Vessel Experiment, submitted to J. Sci. Expl.

[7] M.H. Kohane and W.A. Tiller, On Intention-Induced Increase of In Vitro Enzyme Thermodynamic Activity, submitted to Alternative Therapies in Health and Medicine.

[8] W.A. Tiller, W.E. Dibble, Jr., and M.J. Kohane, Towards Objectifying Intention via Electronic Devices, submitted to Subtle Energies and Energy Medicine.

[9] W.A. Tiller, M.J. Kohane and W.E. Dibble, Jr., Can an Aspect of Consciousness be Imprinted Into an Electronic Device? Submitted to Journal of Consciousness Studies.

[10] M.J. Buerger, "Crystal Structure Analysis" (John Wiley & Sons, Inc., New York 1960) Ch. 15.

[11] R. Bracewell, "The Fourier Transform and Its Applications" (McGraw-Hill Book Company, New York, 1965).

[12] J. Komrska, The Fourier Transform of Lattices, Proceedings of the International Summer School on Diagnostics and Applications of Thin Films, May 27-June 5, 1991, Czechoslovakia (IOP Publishing Ltd.).

[13] I.J.R. Aitchison and A.J.G. Hey, "Gauge Theories in Particle Physics" (Adam Hilger Ltd., Bristol, 1982) p.11.

[14] P.W. Milonni, "The Quantum Vacuum" (Academic Press, Inc., New York, 1994) p.310.

[15] W.A. Tiller, E.E. Green, P.A. Parks and S. Anderson, Towards Explaining Anomalously Large Body Voltage Surges on Exceptional Subjects: Part I, The Electrostatic Approximation, J. Sci. Expl. 9 (1995) 331.

[16] J.W. Gibbs, "The Collected Works, Vol. I" (Yale University Press, New Haven, 1957 Ed).

[17] L. Dossey, "Healing Words: The Power of Prayer and the Practice of Medicine" (Harper Collins, San Francisco, 1993).

[18] H. Benson and M. Stark, "Timeless Healing, The Power and Biology of Belief" (Scribner, New York, 1996).

[19] J.D. Kraus and K.R. Carver, "Electromagnetics" (McGraw-Hill Book Co., Inc., New York, 1973).

[20] J.D. Jackson, "Classical Electrodynamics" (John Wiley & Sons, Inc., New York, 1963).

[21] K. Pribram, "Brain and Perception, Holonomy and Structure in Figural Processing" (Lawrence Erlbaum Associates, Hillsdale, NJ, 1991).

Figure Captions

1. Circuit diagrams for single and three-oscillator devices used as host devices for intention imprinting.

2. Schematic drawing of experimental set-up used in simultaneous device exposure and pH measurement experiments.
3. Experiment configuration utilized in the Fruit Fly Experiments. The study involved three simultaneous experimental variants with respect to the control culture (C) : (1) an identical culture in a Faraday Cage with no device present (F), (2) the same as (1) but with an unimprinted device at cage center present (d,o) and (3) the same as (1) but with an imprinted device at cage center present (d,j).

4. Experiment configuration utilized in the alkaline phosphatase activity study. (a) A core experimental system comprising 100 ml empty quartz tubes placed in beakers containing100 ml pure H2O was utilized for the initial treatment and (b) ALP solution was added to the quartz tubes for the secondary exposure.

5. pH vs. time for stirred undiluted Evian water with 30-minute device exposure.

6. pH vs. time for 50/50 dilution of Castle Rock water with ASTM Type I purified H_20 with simultaneous 2-4 hr. exposure to 3-oscillator imprinted device. Measurements made on (a) large circles, 6/23/97, 2 hr. exposure, (b) crosses, 7/13/97, 4 hr. exposure, (c) small circles, 7/20/97, 2.5 hr. exposure. The dynamic pH values enter the equilibrium range in just a few minutes after the electrode is placed in unstirred solution and remain in this

range for months in the absence of exposure to imprinted devices or to solutions previously exposed to imprinted devices.

7. pH vs. time for 50/50 dilution of Castle Rock water with ASTM Type I purified water. (a) exposure to an unimprinted 3-oscillator device on 7/7/97. (b) exposure to an imprinted 3-oscillator device on 8/5/97.

8. pH vs. time for 50/50 dilution of Castle Rock water with ASTM Type I purified water. Exposure to an imprinted 1-oscillator device with simultaneous pH measurement for the data points depicted by squares but 5 day pre-exposure followed by subsequent pH measurement for data points depicted by circles.

9. pH vs. time for 100% ASTM Type I purified water simultaneously exposed to an imprinted device with pH-increasing intention.

10. Temperature and pH versus time plots for vessel at location B. Vessel at location B contained 250 ml pure water and 1 g $ZnCO_3$ crystallites from a commercial source. Vessel at location A, 150 feet away, contained the same $ZnCO_3$ crystallites but was exposed to a pH-lowering imprinted device. pH measurements at B began two days after the IIED was powered at location A.

11(a). Modulus versus frequency plot from Fourier analysis using data set shown in inset. The fundamental frequency of these highly periodic oscillations is 64 minutes. Data shown is for vessel at location B containing $ZnCO_3$ crystallites, 115 feet from a vessel

at another location (location C) also containing $ZnCO_3$ crystallites and exposed to a pH-lowering imprinted device.

11(b). Close-up of data shown in inset of figure 11a. Note highly periodic nature of this pH data as indicated by data points marked by arrows. The sample interval is one minute.

12(a). pH vs. time plots for vessels at two locations B and C about 115 feet apart. Both vessels contain pure water and $ZnCO_3$ crystallites but only vessel at location C is exposed to a pH-lowering imprinted device about one foot away. The sample interval is one minute.

12(b). Continuation pH vs. time plots for vessels at locations B and C.

13. pH vs. time plots for vessels at the same two locations B and C illustrating effects of shaking on pH-time course and development of short-period oscillations.

14(a). Temperature and pH versus time plots for vessel at location B for another experiment. Again, a vessel at location C (data not shown) is exposed to a pH-lowering imprinted device about one foot away. The sample interval is one minute.

14(b). Close-up of data shown in figure14a illustrating in-phase coupling between pH and temperature.

15(a). Temperature and conductivity versus time plots for 0.01 M $MgSO_4$ solution exposed to conditioned environment where strong R-space coupling is present (see figure 18). Temperature is measured using high-resolution digital thermometer. Conductivity and temperature are measured simultaneously in the same solution. In-phase correlation between temperature and conductivity is illustrated.

15(b). Temperature and pH versus time plots for 0.01 M KCl solution exposed to conditioned environment where strong R-space coupling is present (see figure 18). Temperature is measured using high-resolution digital thermometer. In this experiment, in-phase correlation between temperature and pH is illustrated using a different solution.

16(a). Larval development time for the four treatments, (C), (F), (d,j), and (d,o). The corresponding ANOVA is given in Table 1.

16(b). [ATP]/[ADP] ratio in the presence of 0.01 Molar NAD. The corresponding ANOVAs are given in Table 1.

17. ALP activity for the four treatments, (C), (F), (d,j), and (d,o). The ALP dilutions were:

dilution 1 - 100ul ALP solution plus 150 µl pure H20

dilution 2 - 100ul ALP solution plus 200 µl pure H20

18. A visualization of dual four-space frames (physical or D-space and conjugate physical or R-space) imbedded in a nine-space (emotion frame) imbedded in a ten-space (mind frame) and all this embedded in an eleven-space (spirit domain).

19. Illustration of one possible process path whereby spirit produces action in the physical domain.

ANOVA FOR THE LARVAL DEVELOPMENT TIME

The population mean for each experiment was treated as the primary data.

df represents the degrees of freedom and F the variance ratio

Treatment effects were significant at $p < 0.001$ and d_j was significantly greater than d_o.

source	df	sum of squares	mean square	F
device/treatment	3	6.103	2.034	19.651**
error	12	1.242	0.104	

** indicates $p<0.001$

ANOVA FOR THE [ATP]/[ADP] RATIO

The population mean for each experiment was treated as the primary data.

df represents the degrees of freedom and F the variance ratio

(a) 0.01 M NAD

source	df	sum of squares	mean square	F
device/treatment	3	0.928	0.309	107.920**
error	28	0.08	0.003	

(b) With Pure Water

source	df	sum of squares	mean square	F
device/treatment	3	0.075	0.03	17.733**
error	28	0.04	0.003	

** indicates $p<0.001$

Table 1

Figure 1

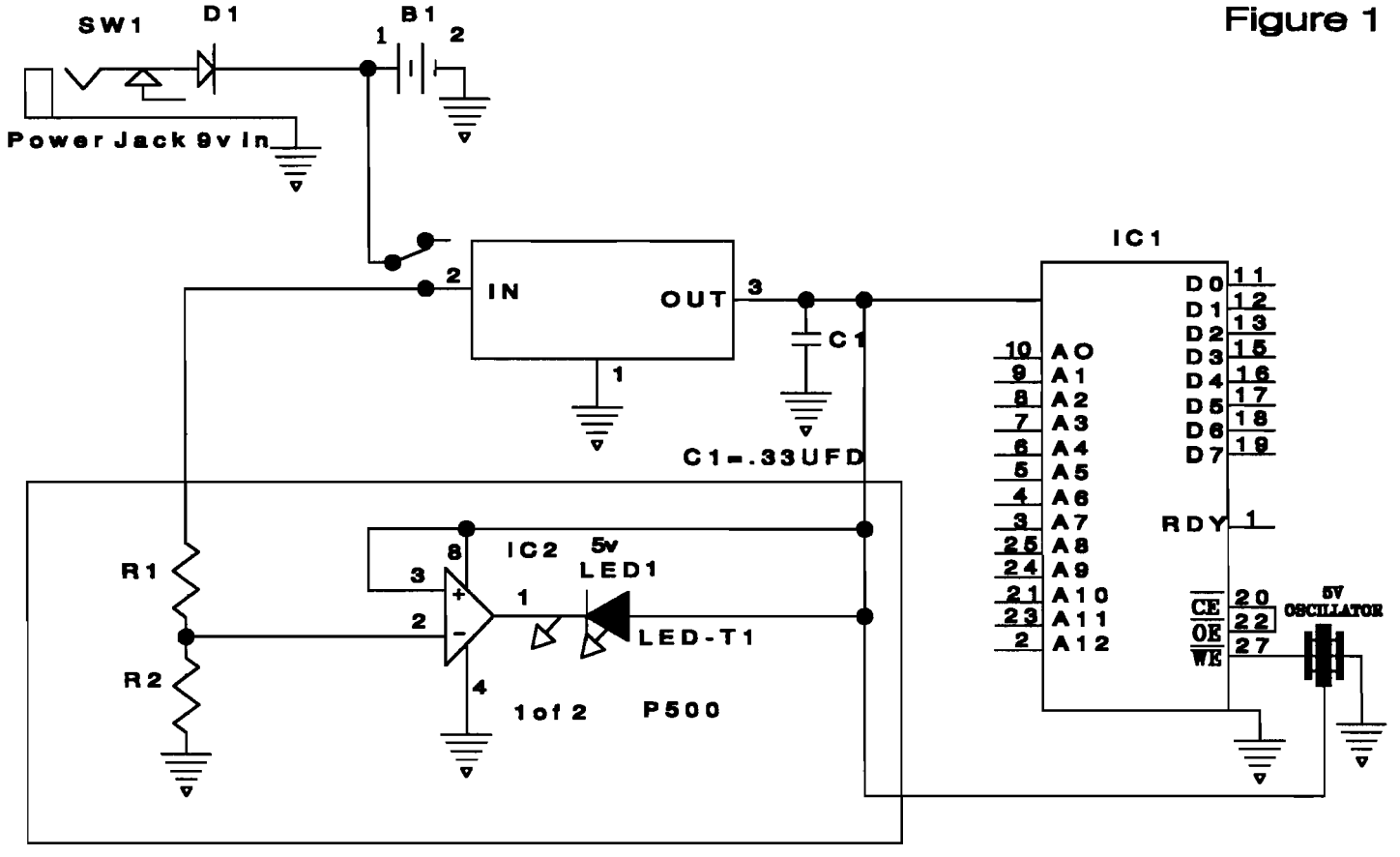
SW1
D1
B1
Power Jack 9v In
IN
OUT
C1
C1=.33UFD
IC1
IC2
5v
LED1
LED-T1
1of2
P500
R1
R2
A0
A1
A2
A3
A4
A5
A6
A7
A8
A9
A10
A11
A12
D0
D1
D2
D3
D4
D5
D6
D7
RDY
CE
OE
WE
5V
OSCILLATOR

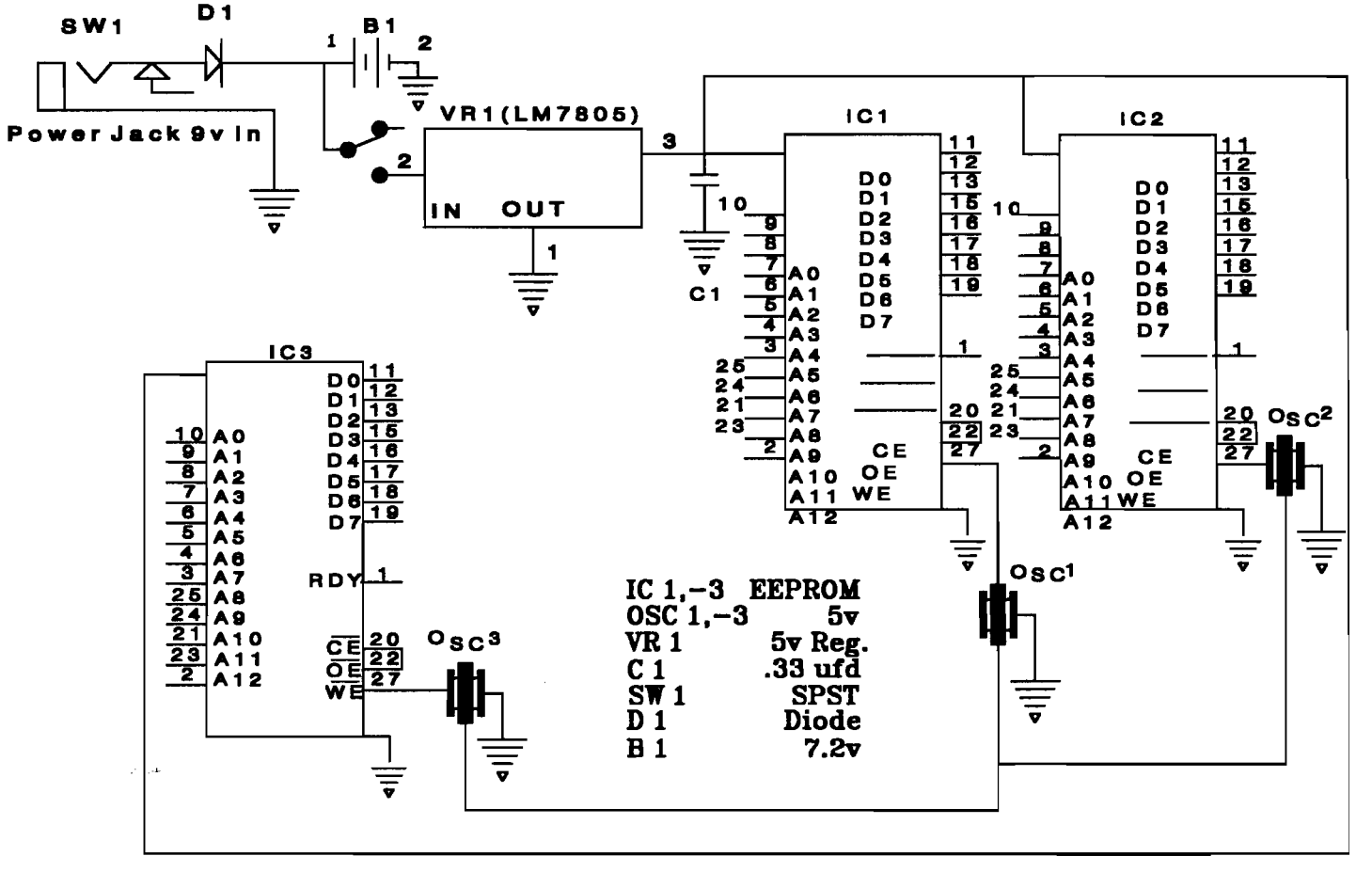
SW1
D1
B1
Power Jack 9v In
VR1(LM7805)
IN
OUT
C1
IC1
IC2
IC3
Osc1
Osc2
Osc3
IC 1,-3 EEPROM
OSC 1,-3 5v
VR 1 5v Reg.
C 1 .33 ufd
SW 1 SPST
D 1 Diode
B 1 7.2v

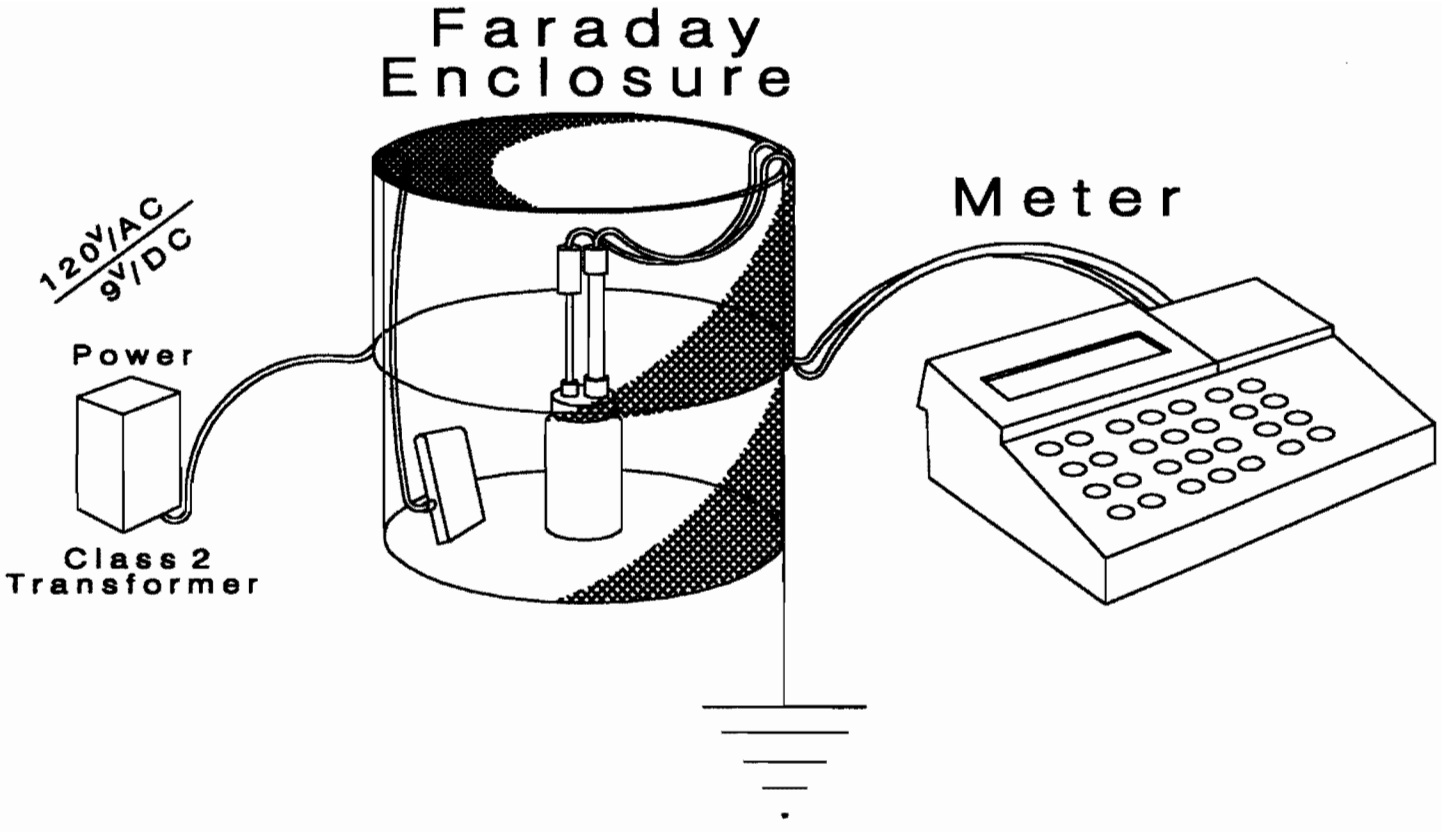

Figure 2

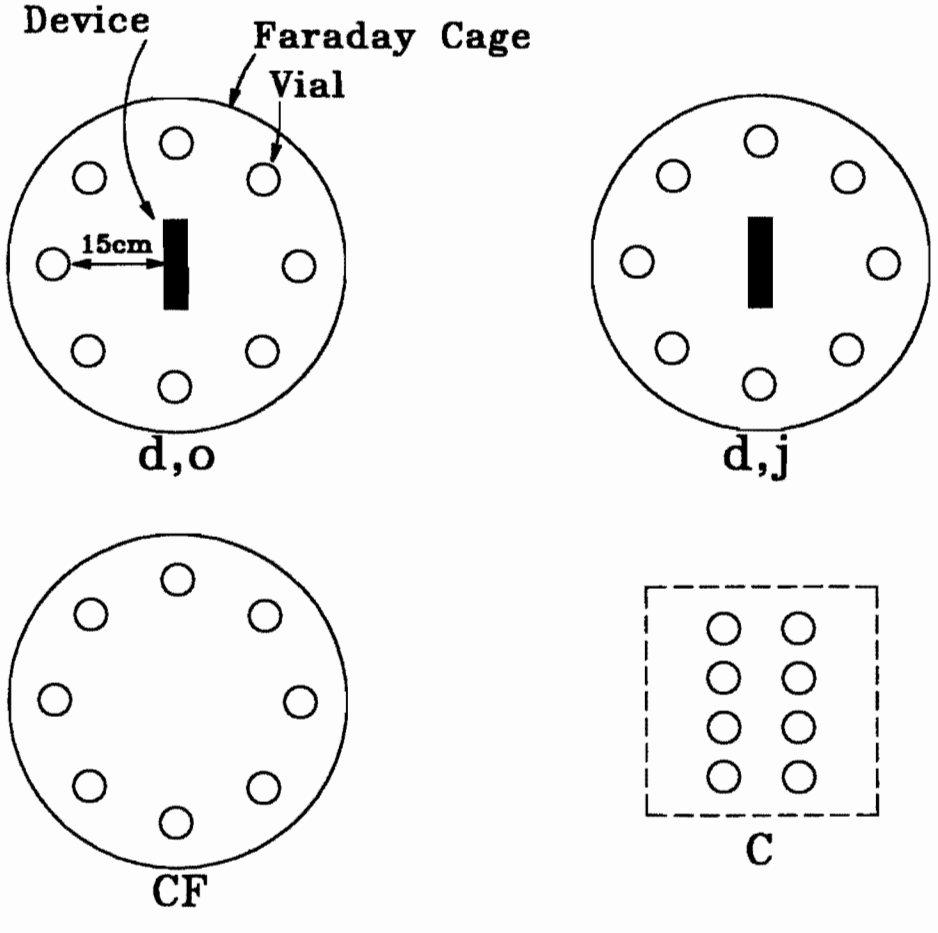

Figure 3

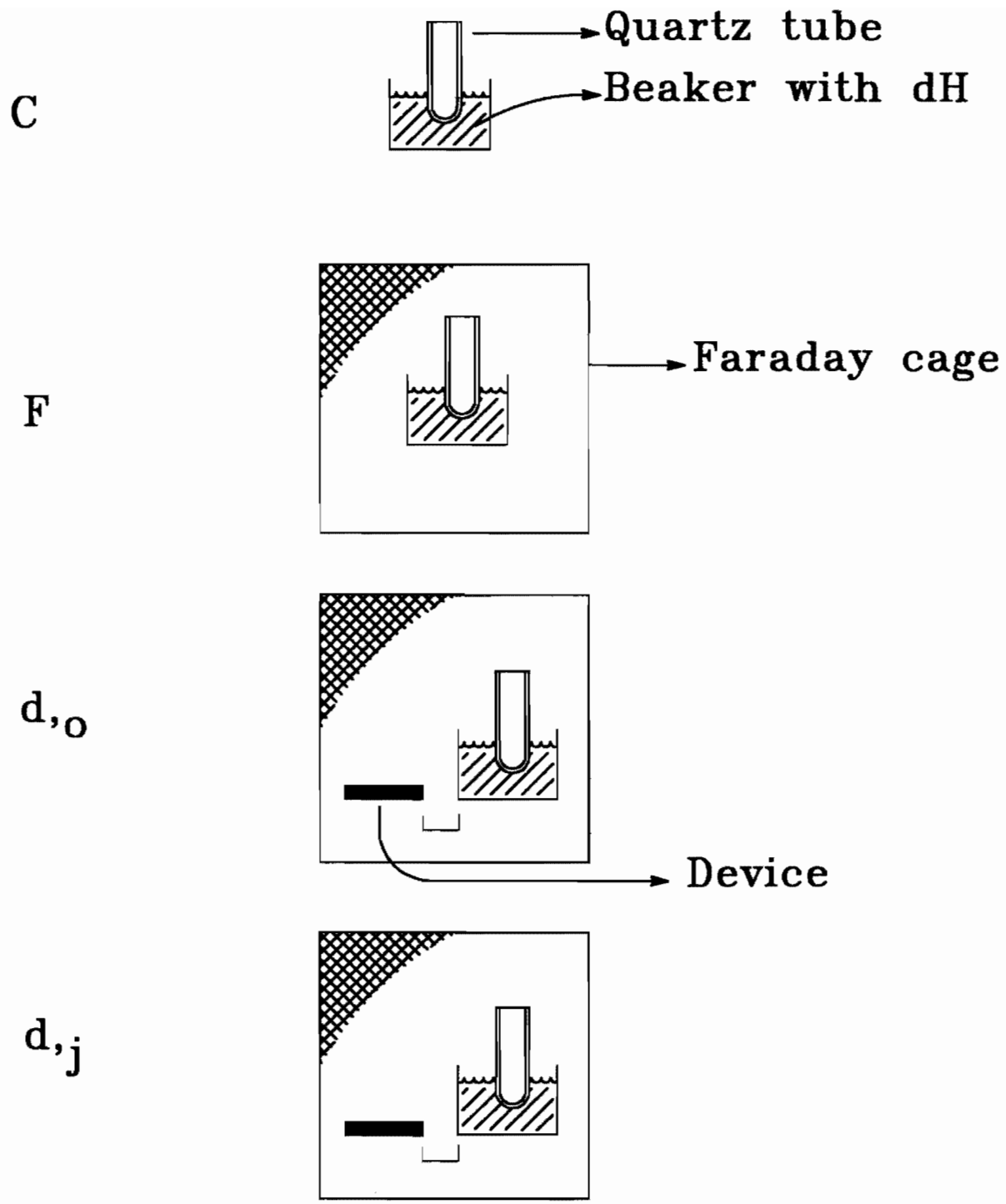
C
Quartz tube
Beaker with dH
F
Faraday cage
d,o
Device
d,j
Scale: ⌴ 2cm

Figure 4(a)

C

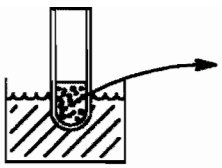

F

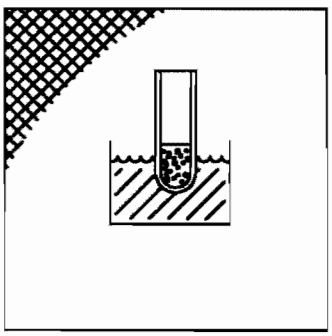

$d_{,o}$

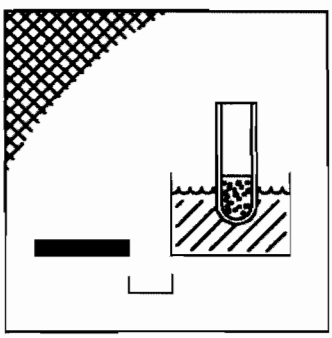

$d_{,j}$

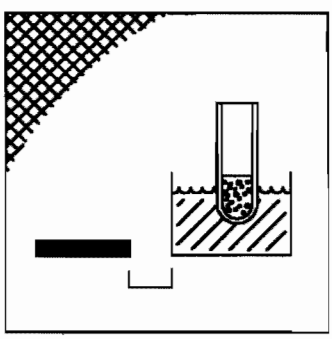

Scale: ⌴ 2cm

Figure 4(b)

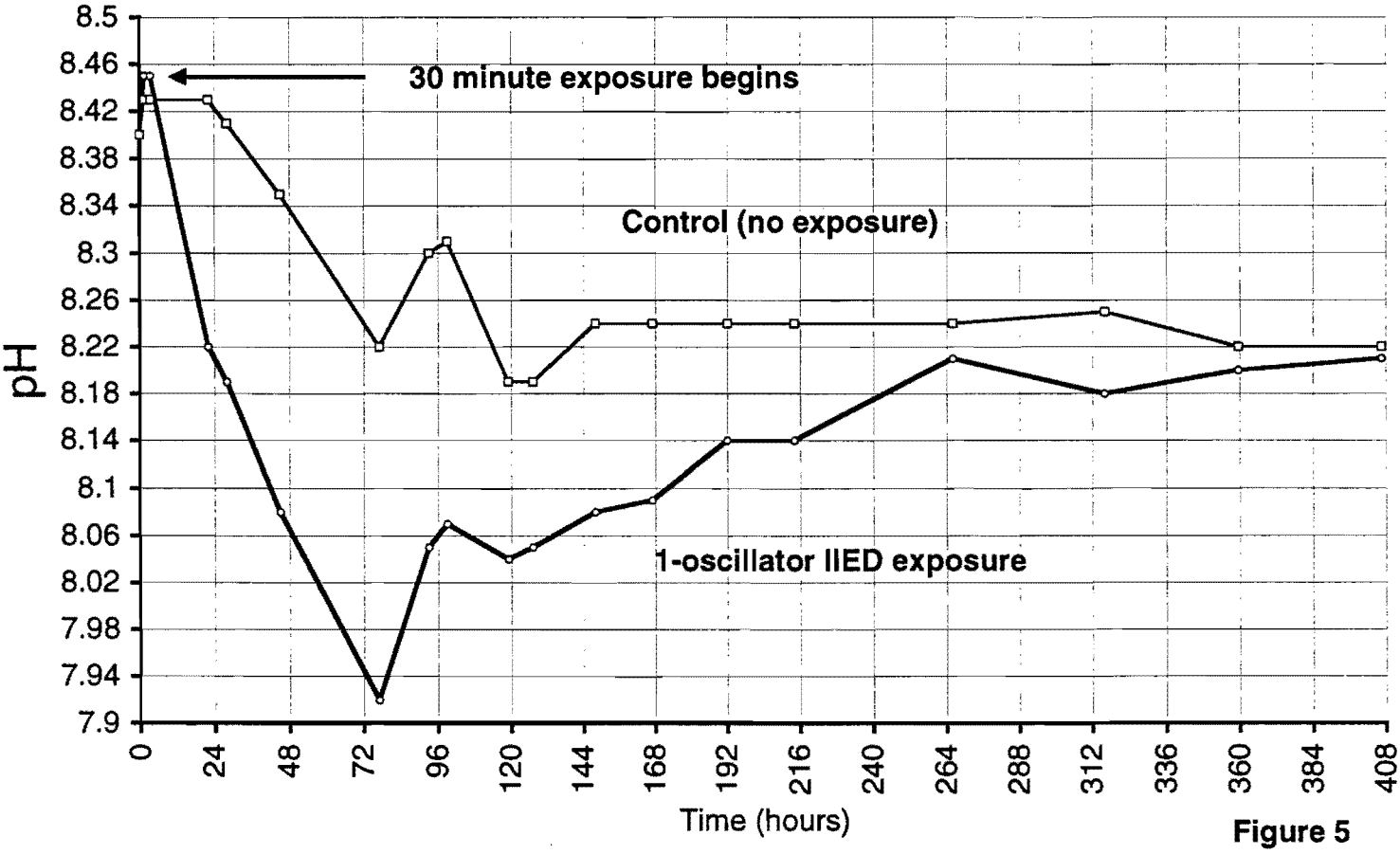

Figure 5

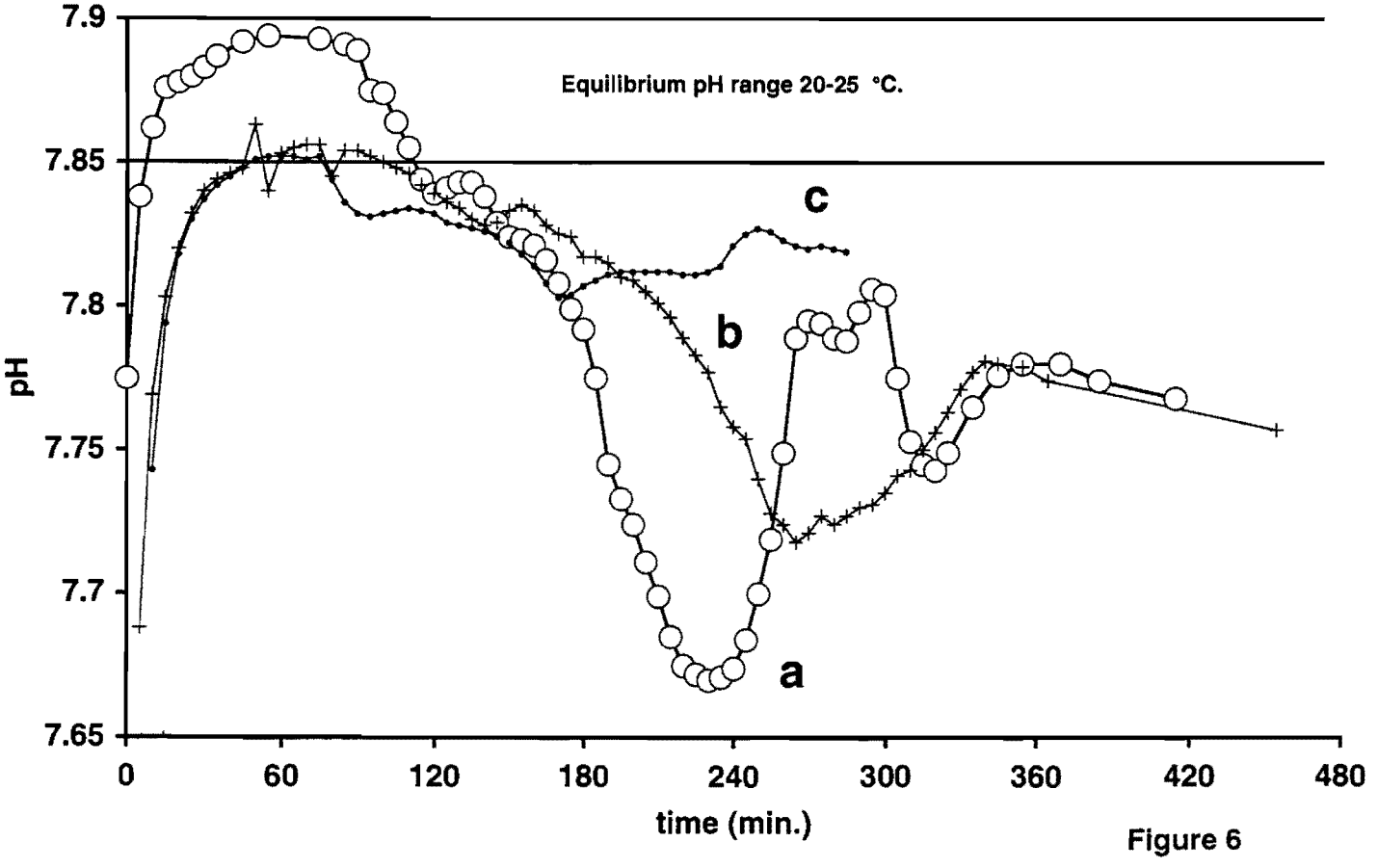

Figure 6

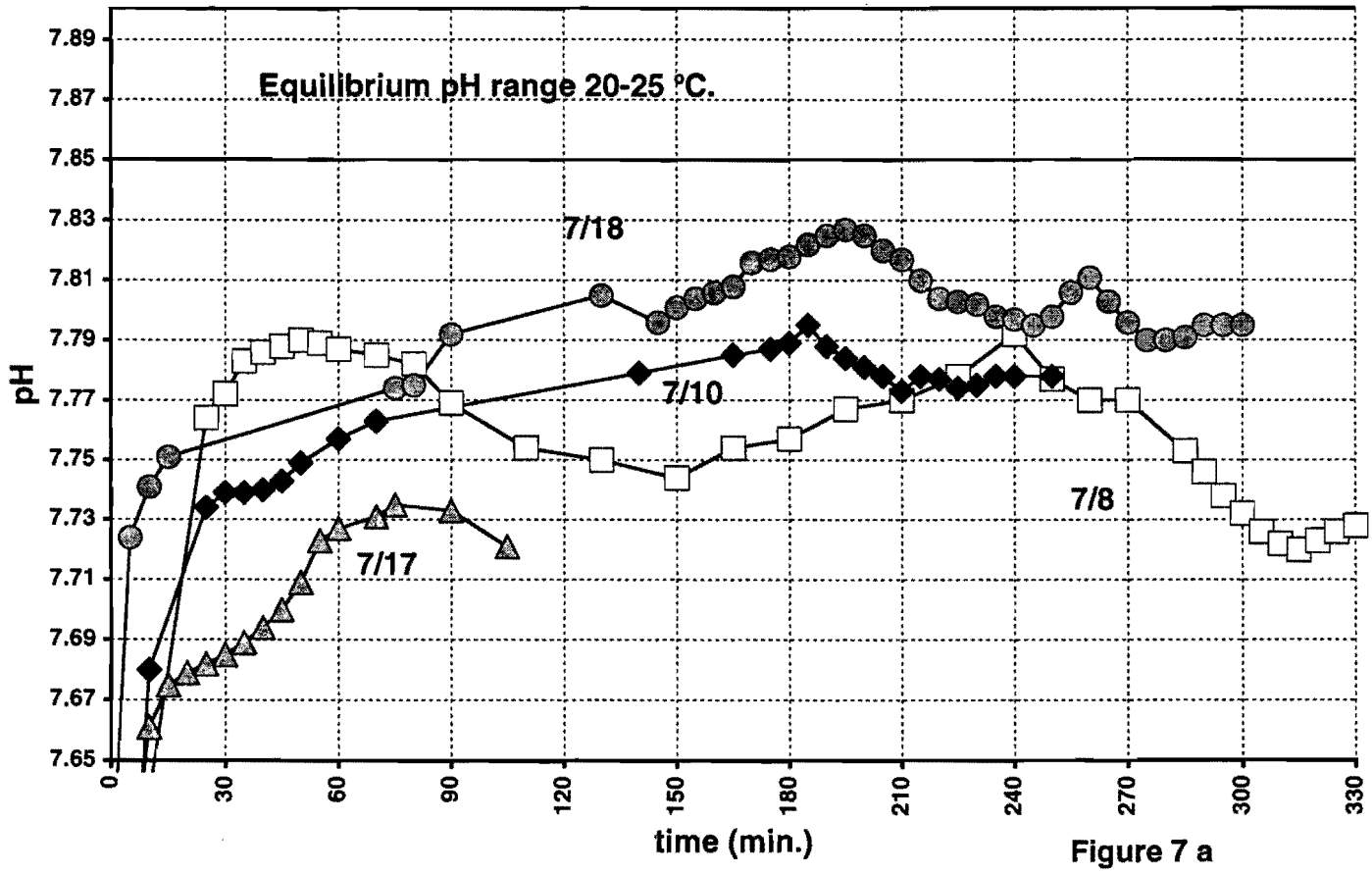

Figure 7 a

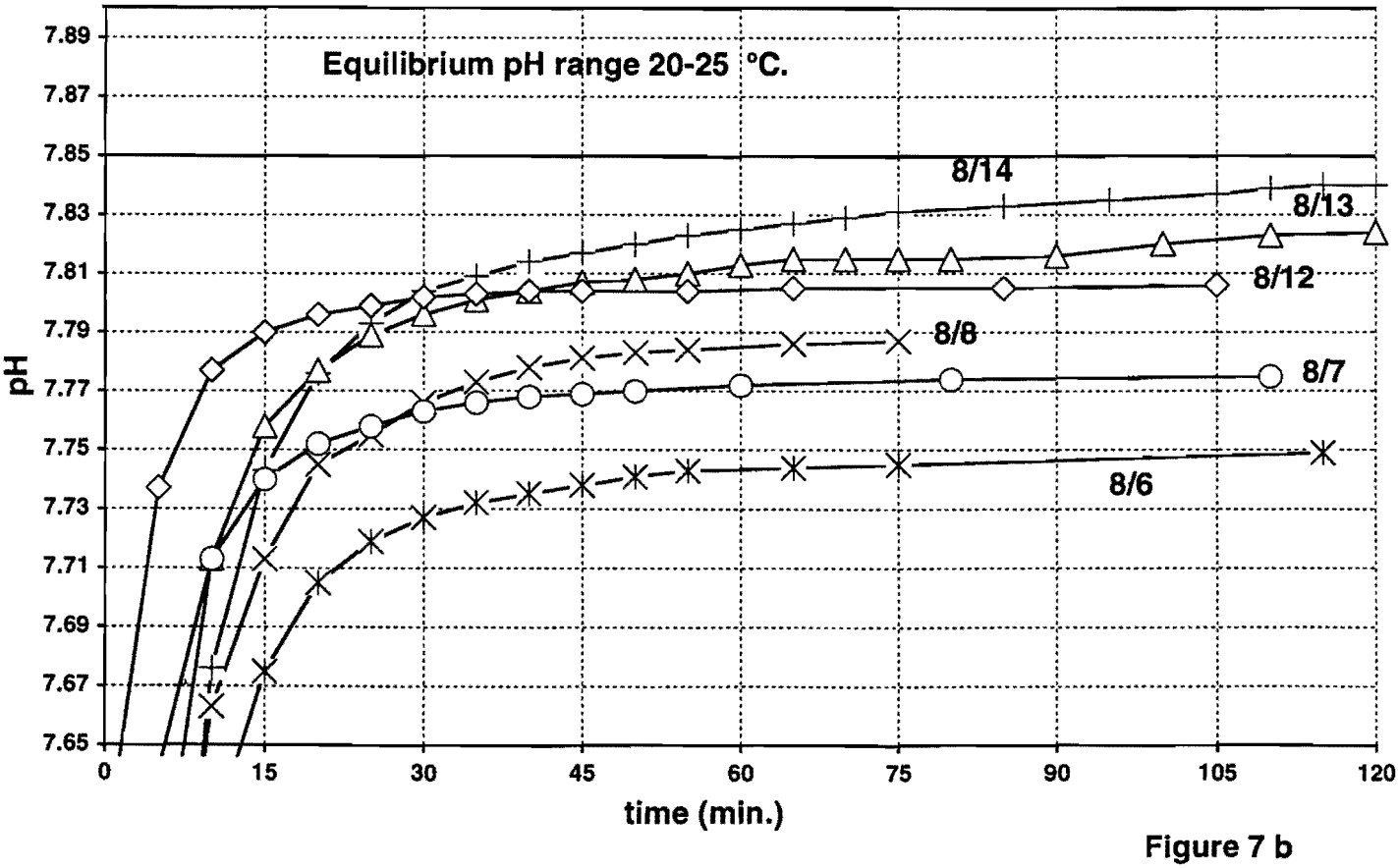

Figure 7 b

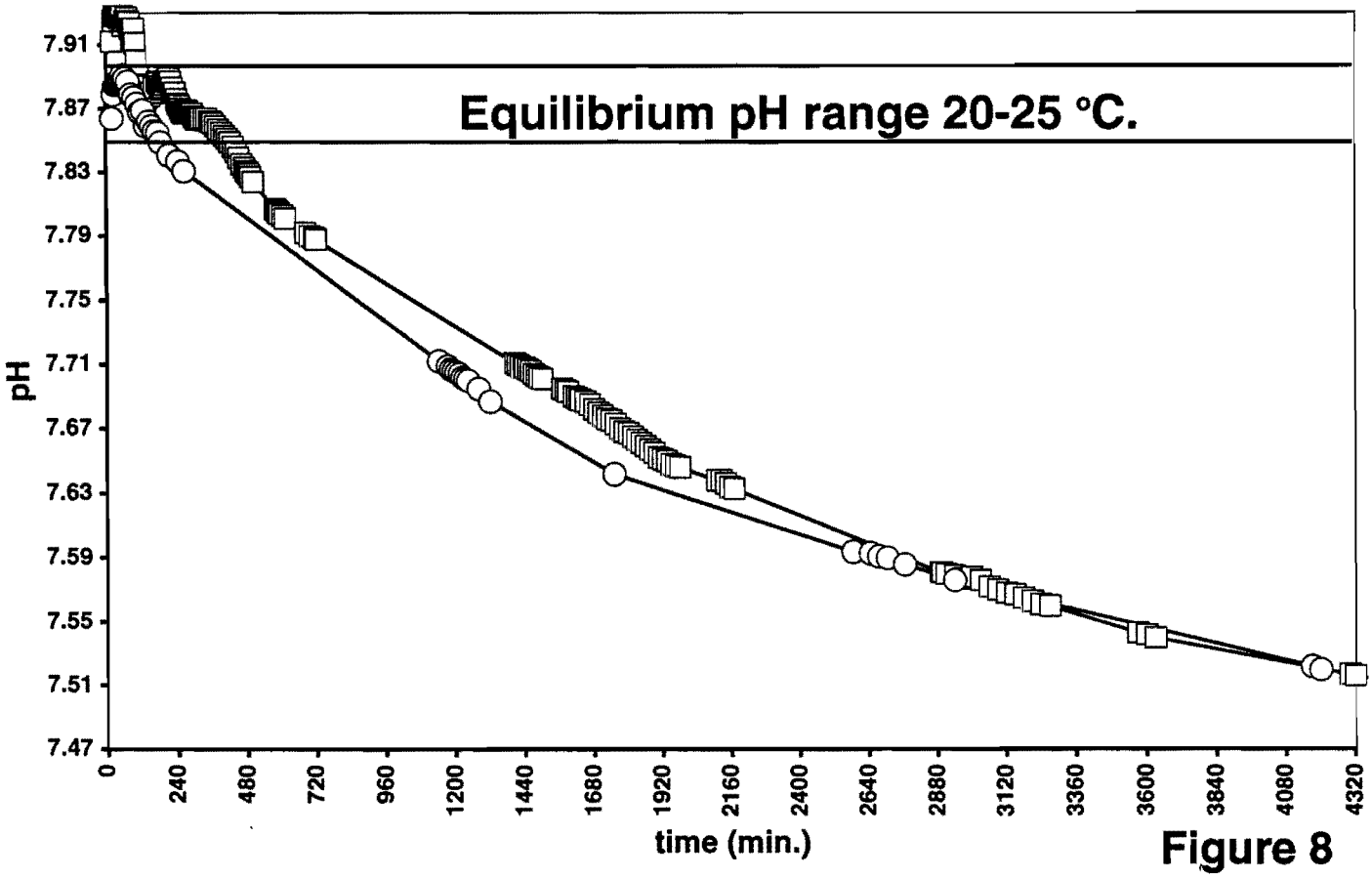

Figure 8

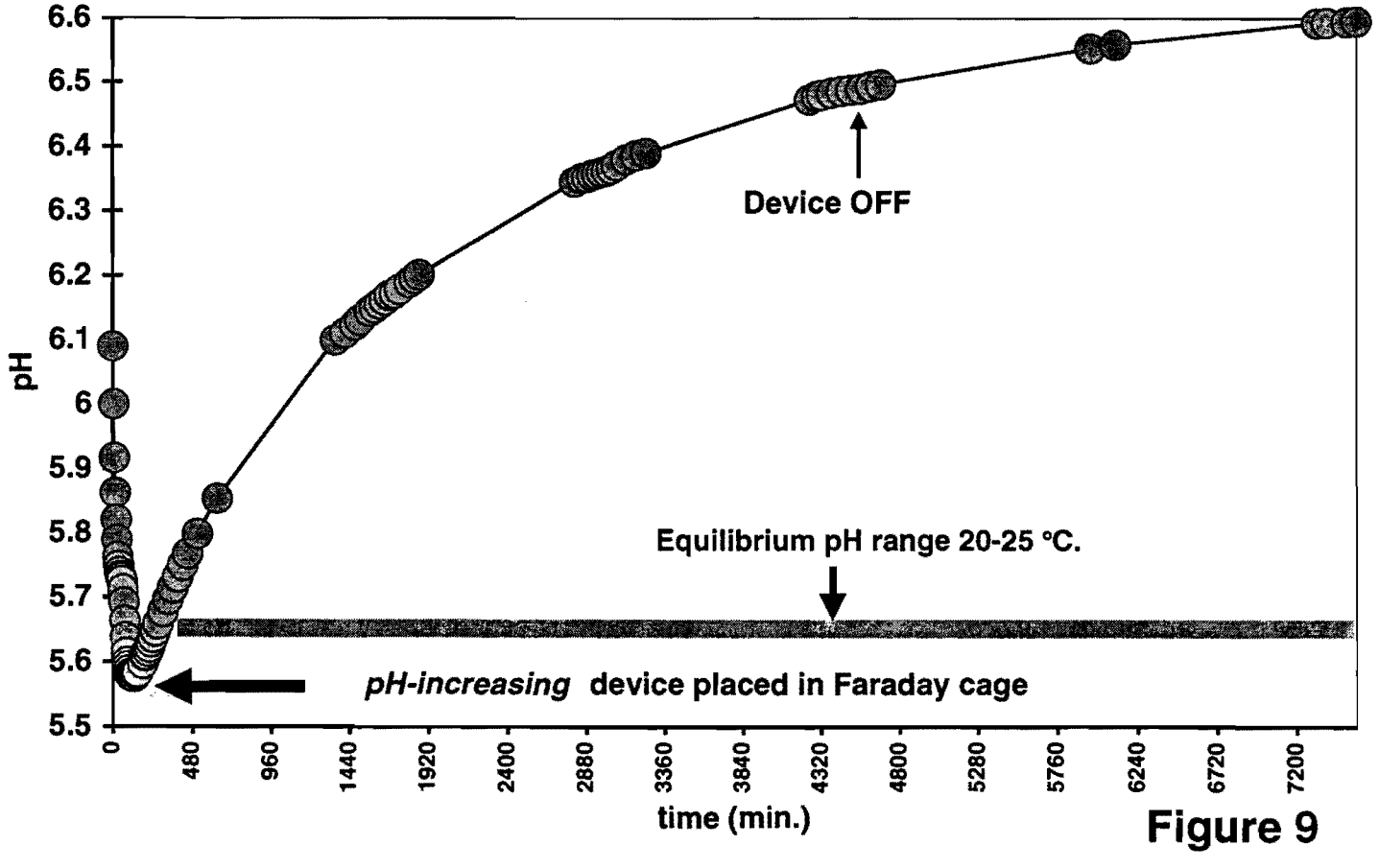

Figure 9

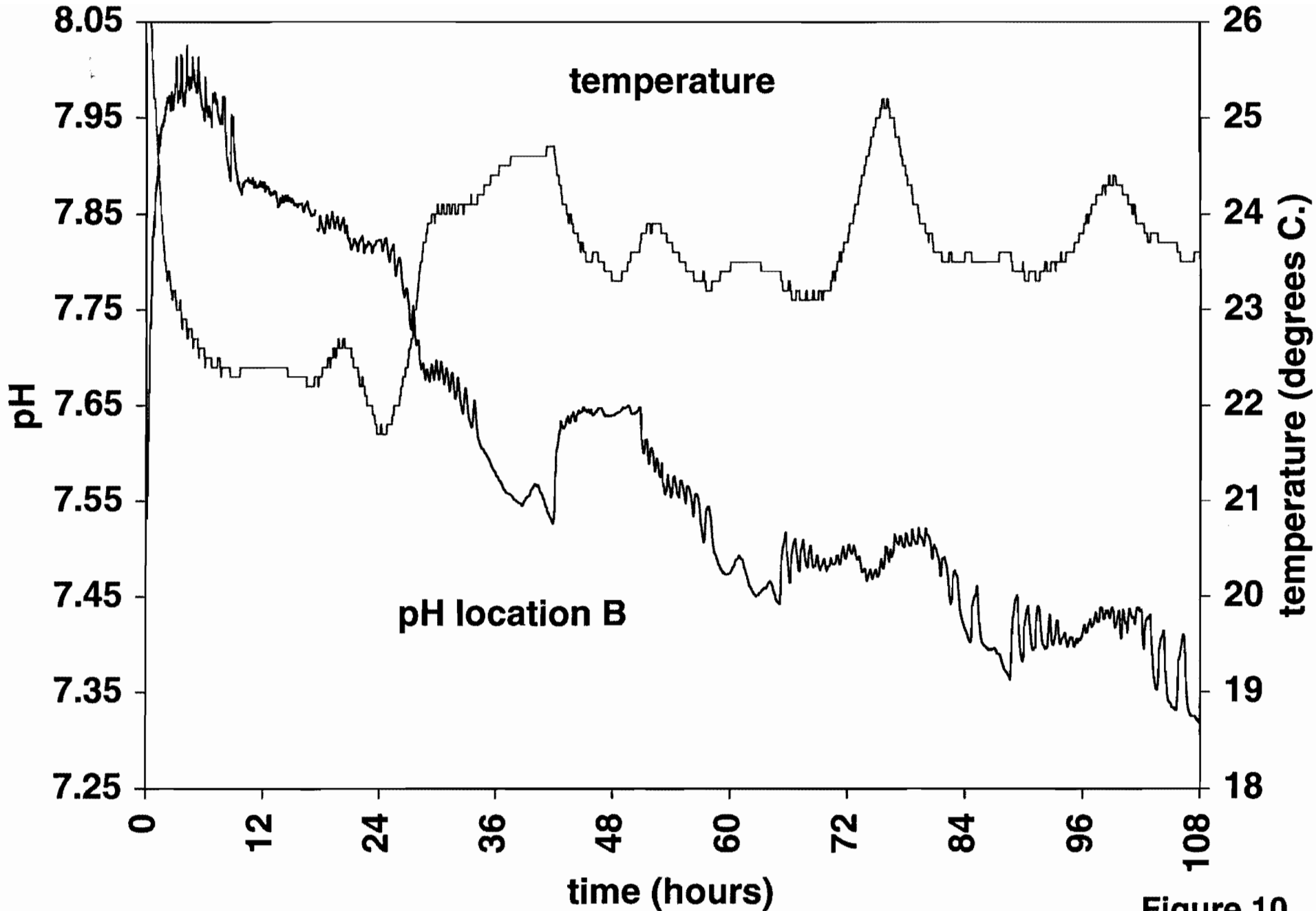
8.05
7.95
7.85
7.75
7.65
7.55
7.45
7.35
7.25
pH
26
25
24
23
22
21
20
19
18
temperature (degrees C.)
temperature
pH location B
0
12
24
36
48
60
72
84
96
108
time (hours)

Figure 10

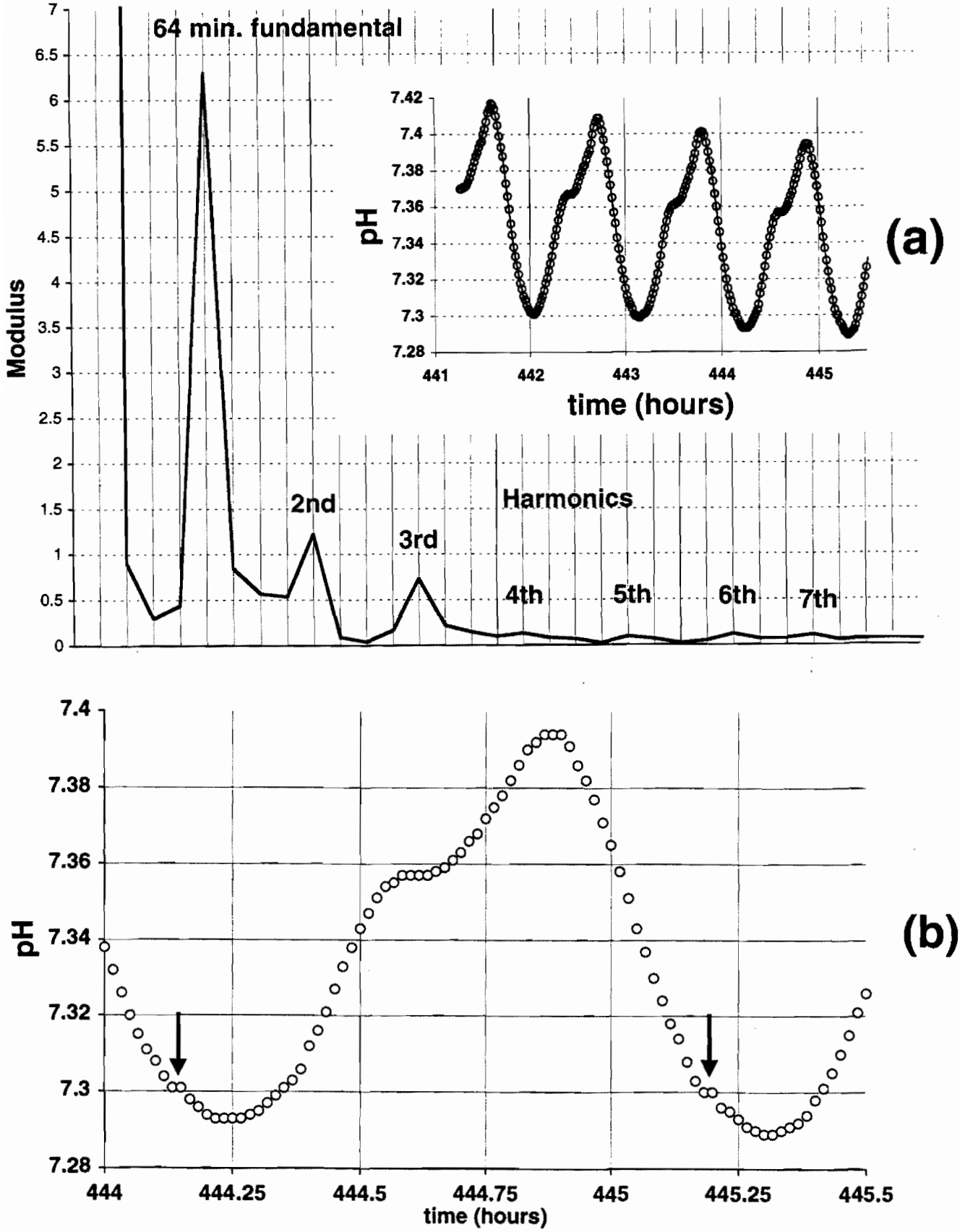
64 min. fundamental
Modulus
7
6.5
6
5.5
5
4.5
4
3.5
3
2.5
2
1.5
1
0.5
0
2nd
3rd
Harmonics
4th
5th
6th
7th
pH
7.42
7.4
7.38
7.36
7.34
7.32
7.3
7.28
441
442
443
444
445
time (hours)
(a)
pH
7.4
7.38
7.36
7.34
7.32
7.3
7.28
444
444.25
444.5
444.75
445
445.25
445.5
time (hours)
(b)

Figure 11

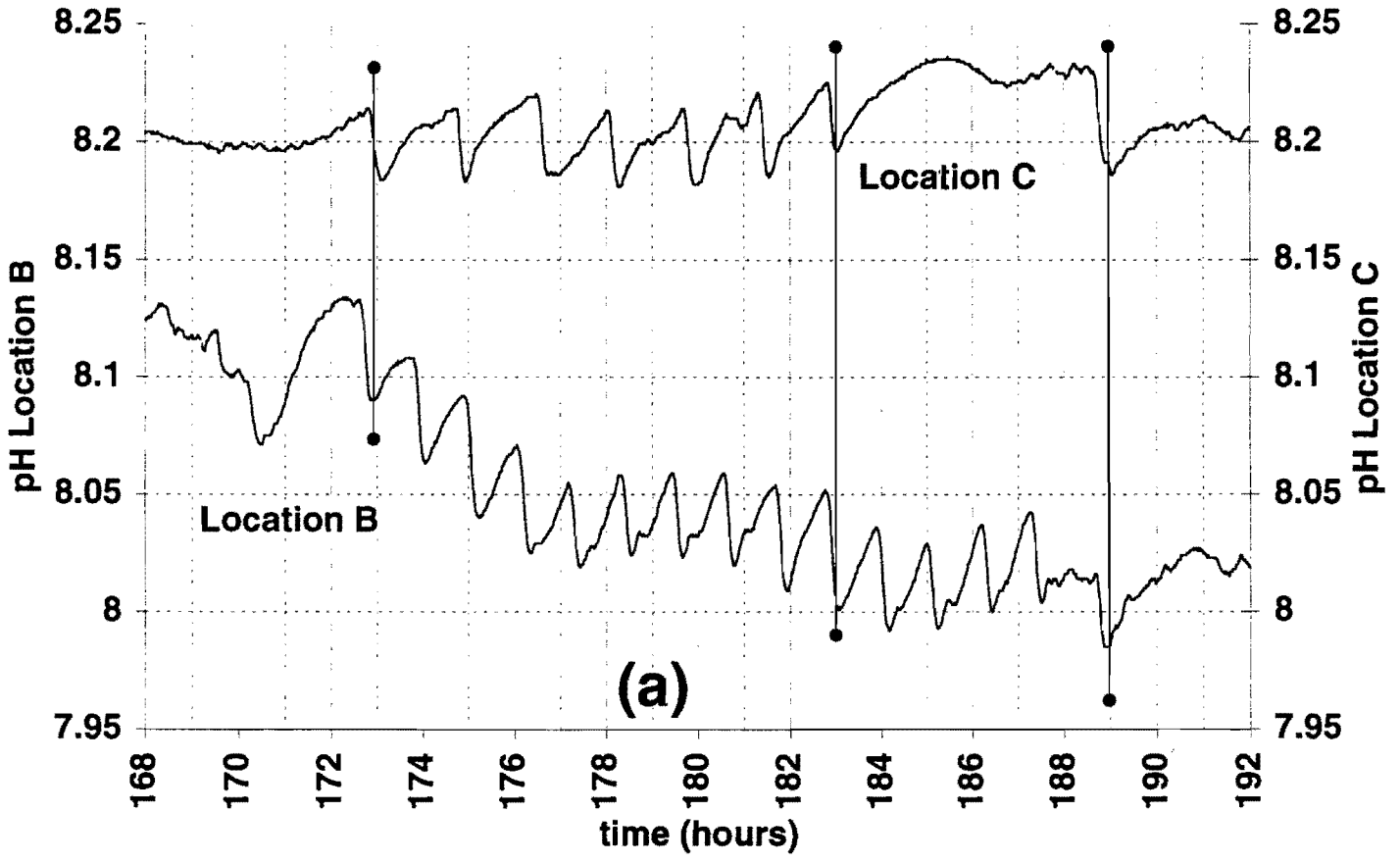
8.25
8.2
8.15
8.1
8.05
8
7.95
pH Location B
pH Location C
Location C
Location B
(a)
168
170
172
174
176
178
180
182
184
186
188
190
192
time (hours)

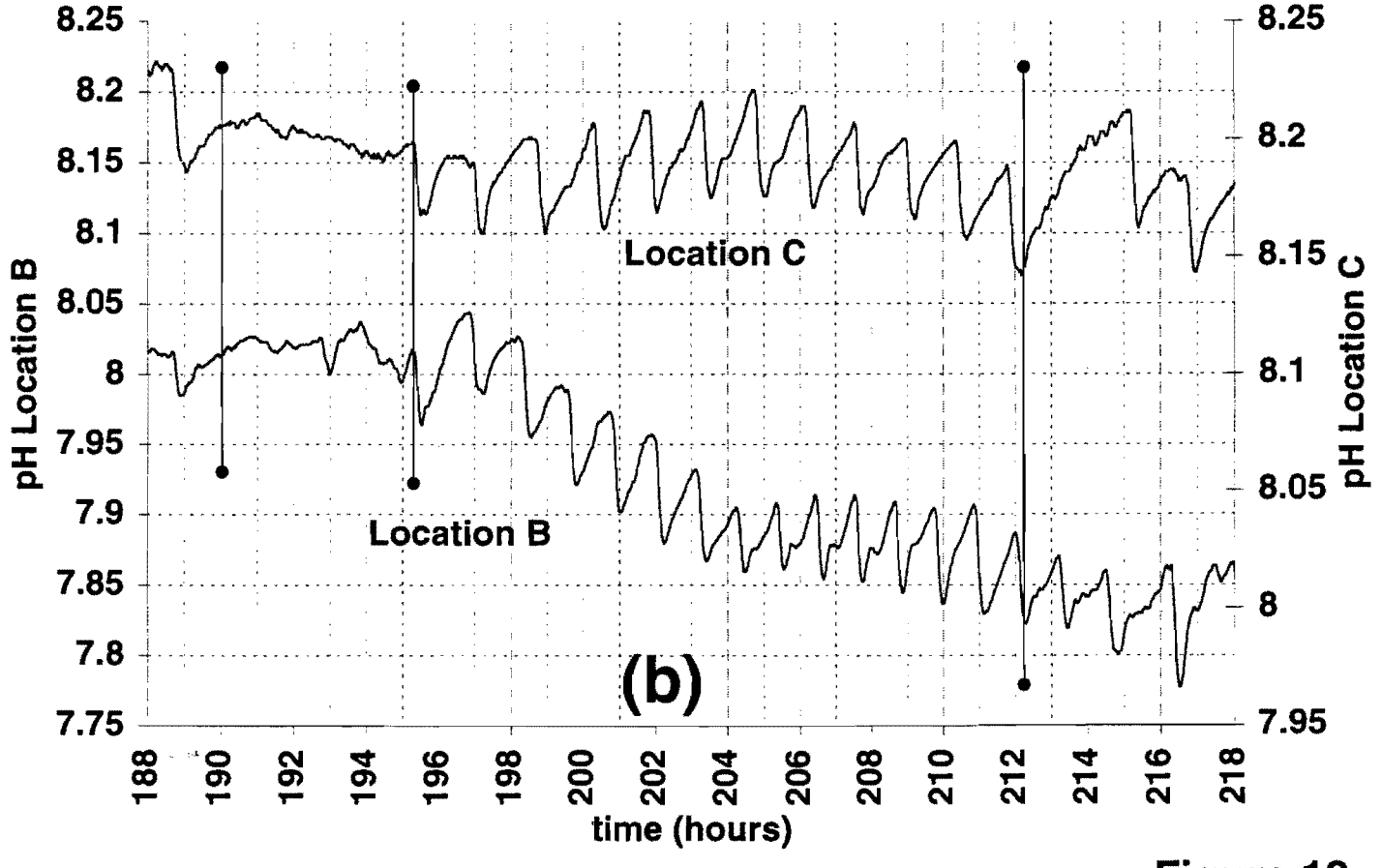
8.25
8.2
8.15
8.1
8.05
8
7.95
7.9
7.85
7.8
7.75
pH Location B
pH Location C
Location C
Location B
(b)
188
190
192
194
196
198
200
202
204
206
208
210
212
214
216
218
time (hours)

Figure 12

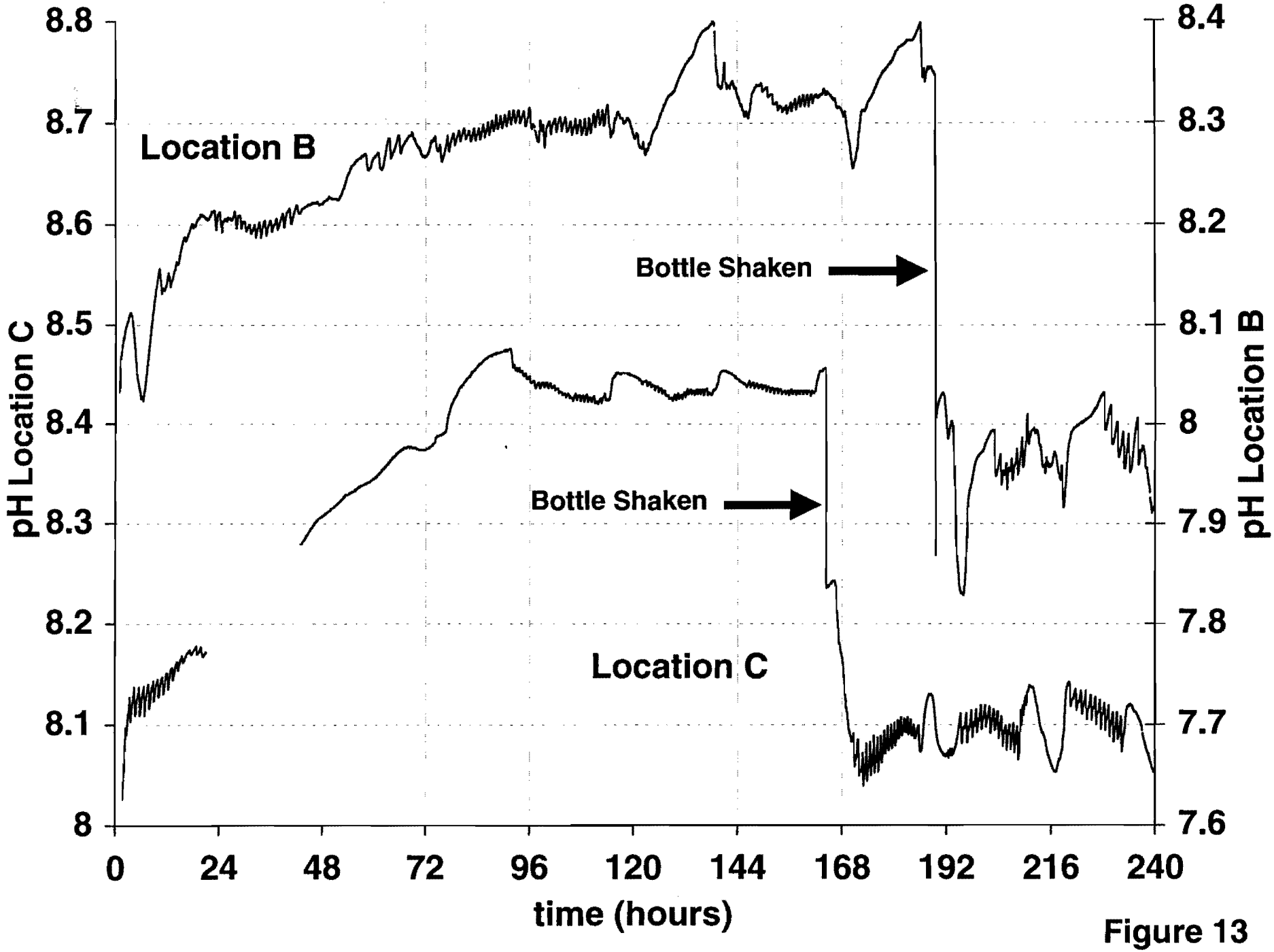
Location B
Bottle Shaken
Bottle Shaken
Location C
pH Location C
pH Location B
time (hours)
8.8
8.7
8.6
8.5
8.4
8.3
8.2
8.1
8
8.4
8.3
8.2
8.1
8
7.9
7.8
7.7
7.6
0
24
48
72
96
120
144
168
192
216
240

Figure 13

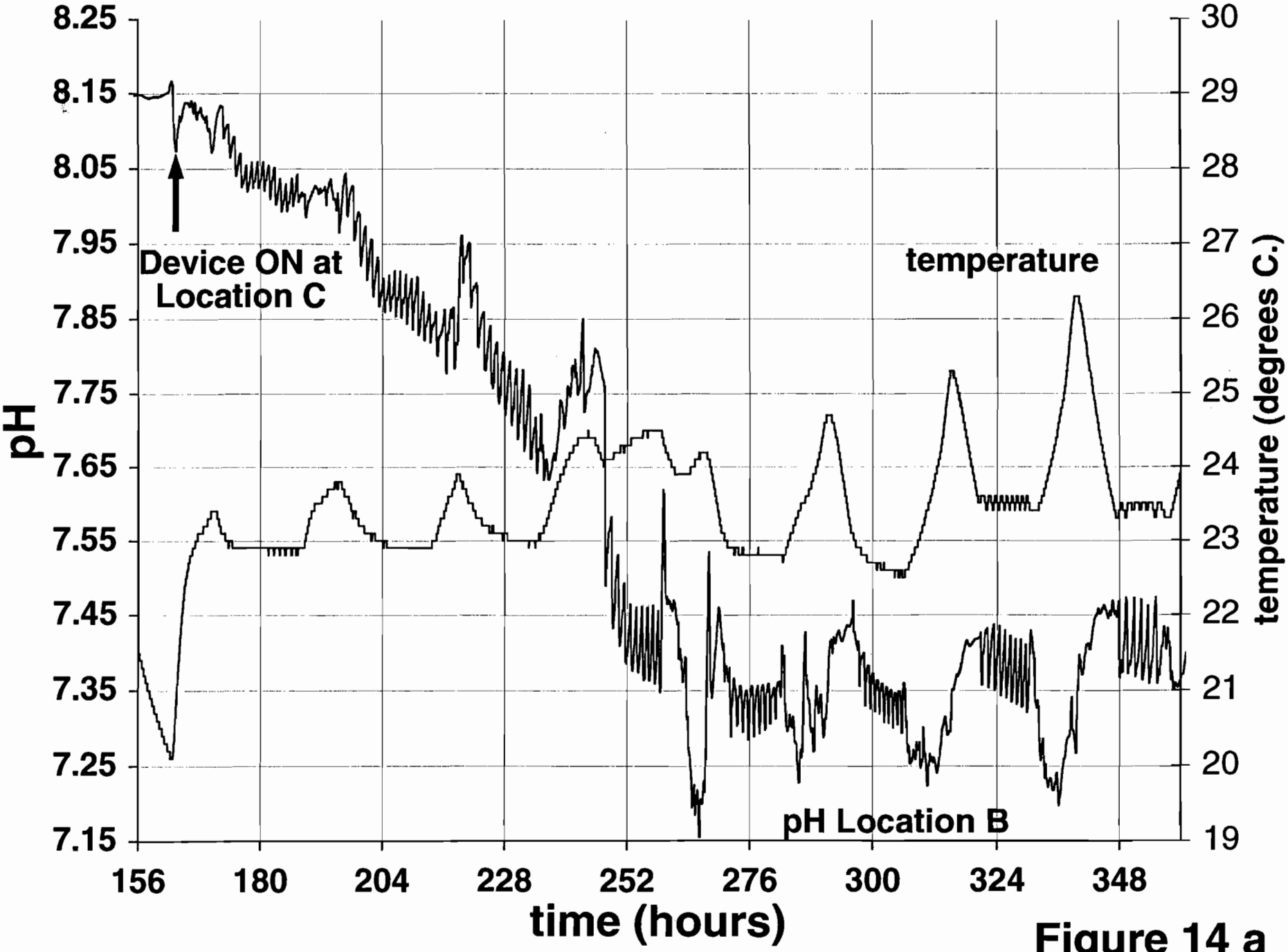
8.25
8.15
8.05
7.95
7.85
7.75
7.65
7.55
7.45
7.35
7.25
7.15
pH
30
29
28
27
26
25
24
23
22
21
20
19
temperature (degrees C.)
Device ON at
Location C
temperature
pH Location B
156
180
204
228
252
276
300
324
348
time (hours)

Figure 14 a

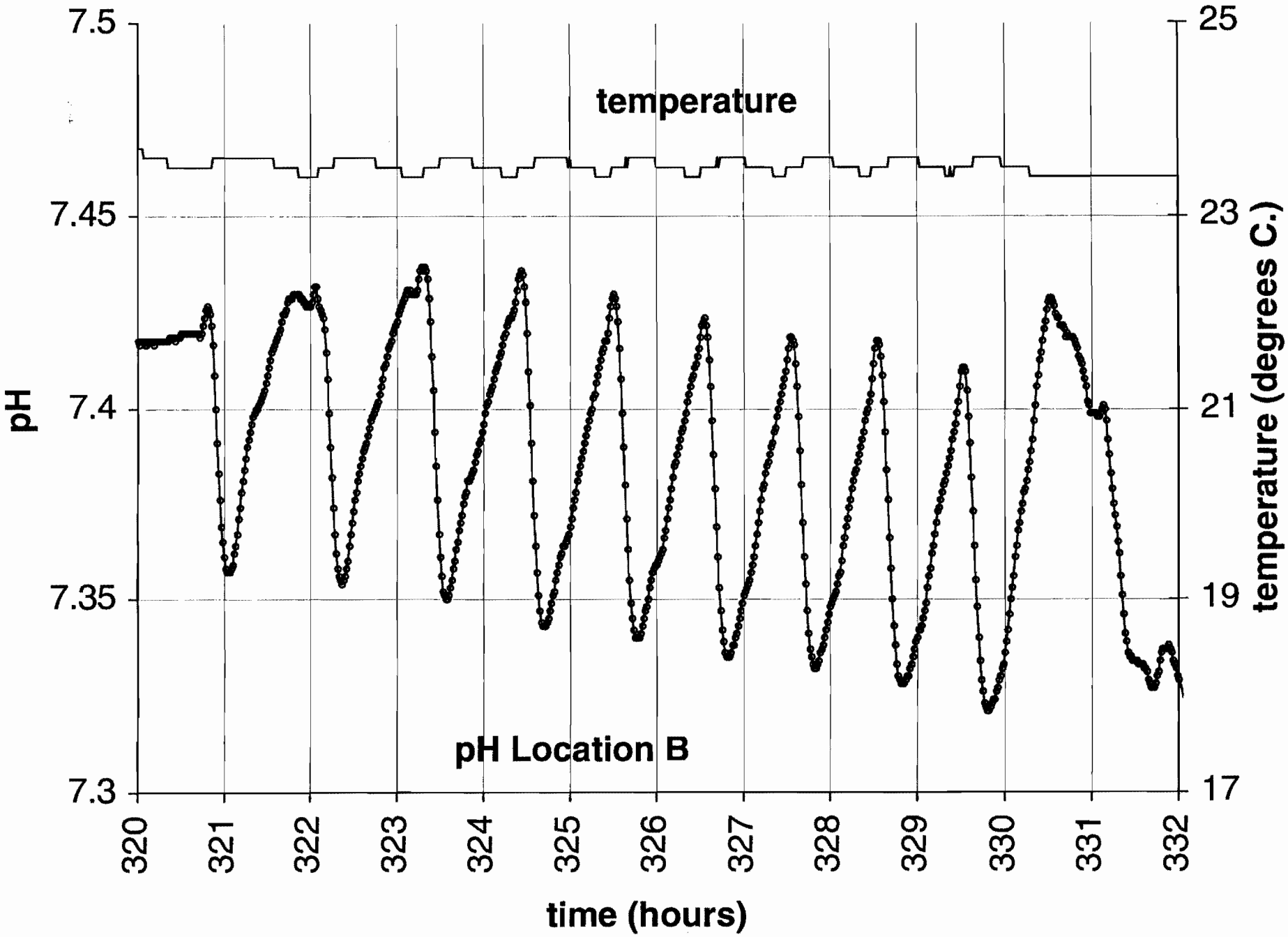
7.5
7.45
7.4
7.35
7.3
pH
25
23
21
19
17
temperature (degrees C.)
temperature
pH Location B
320
321
322
323
324
325
326
327
328
329
330
331
332
time (hours)

Figure 14 b

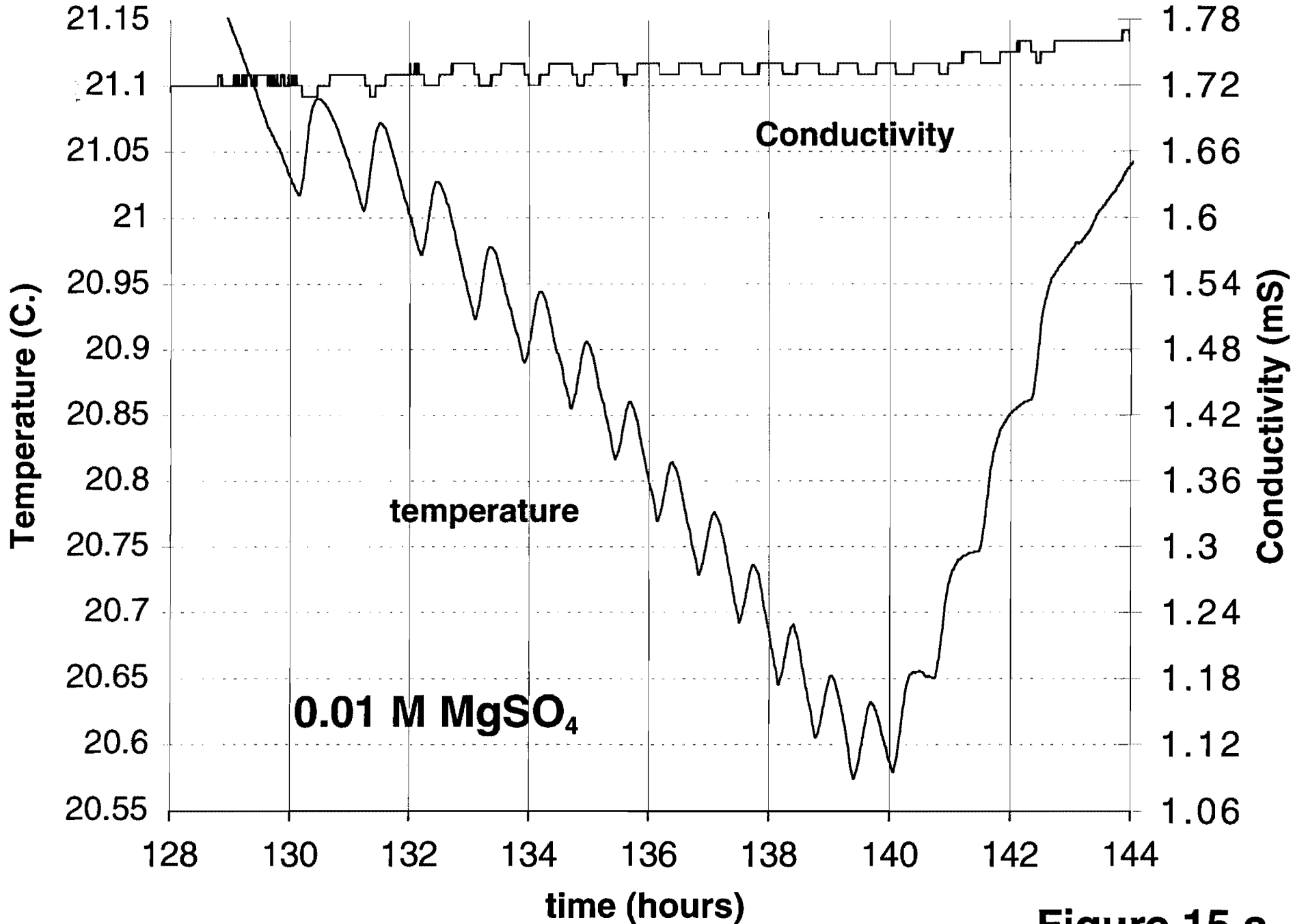
21.15
21.1
21.05
21
20.95
20.9
20.85
20.8
20.75
20.7
20.65
20.6
20.55
Temperature (C.)
1.78
1.72
1.66
1.6
1.54
1.48
1.42
1.36
1.3
1.24
1.18
1.12
1.06
Conductivity (mS)
Conductivity
temperature
0.01 M MgSO4
128
130
132
134
136
138
140
142
144
time (hours)

Figure 15 a

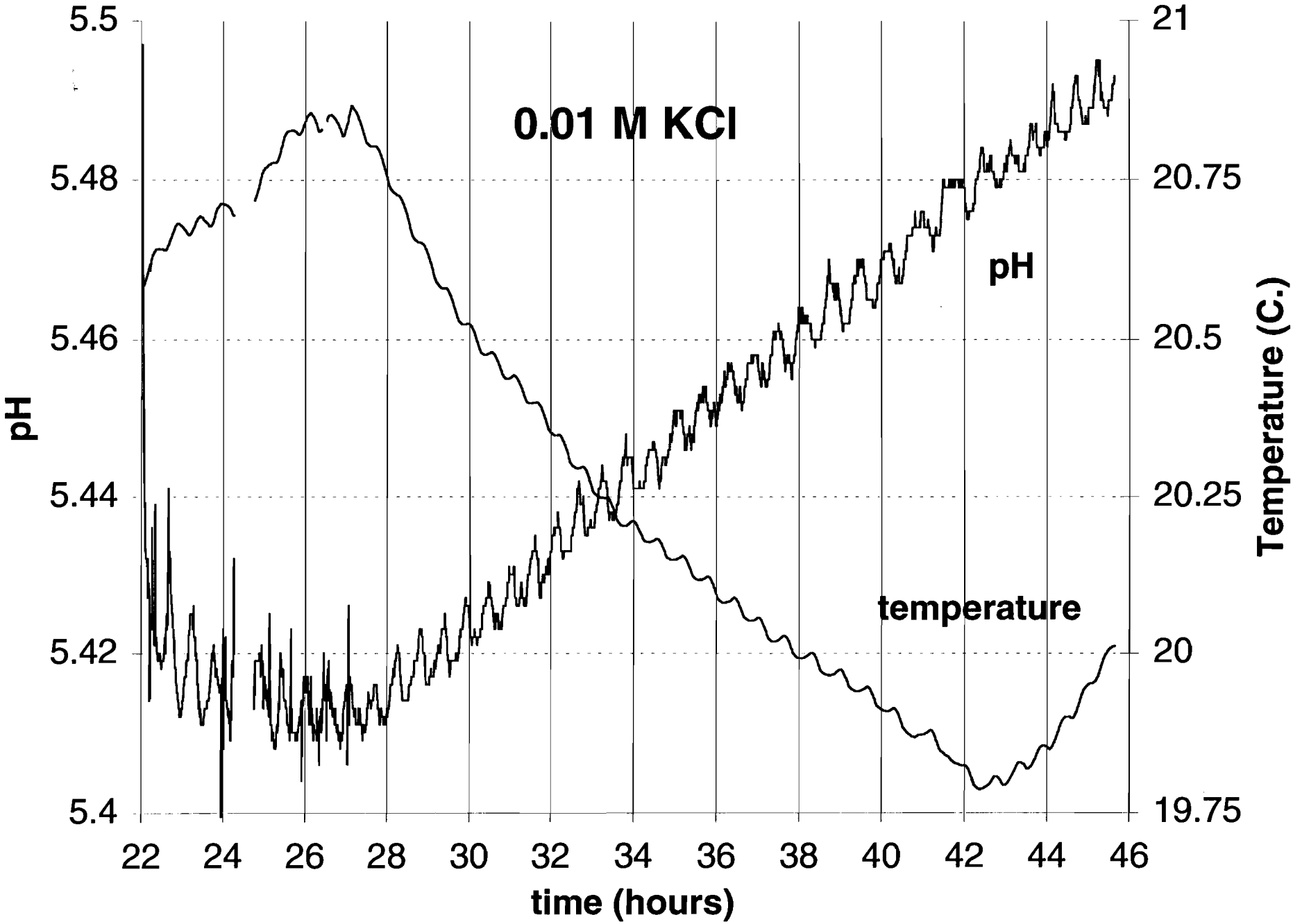
0.01 M KCl
pH
temperature
pH
Temperature (C.)
time (hours)
5.5
5.48
5.46
5.44
5.42
5.4
21
20.75
20.5
20.25
20
19.75
22
24
26
28
30
32
34
36
38
40
42
44
46

Figure 15 b

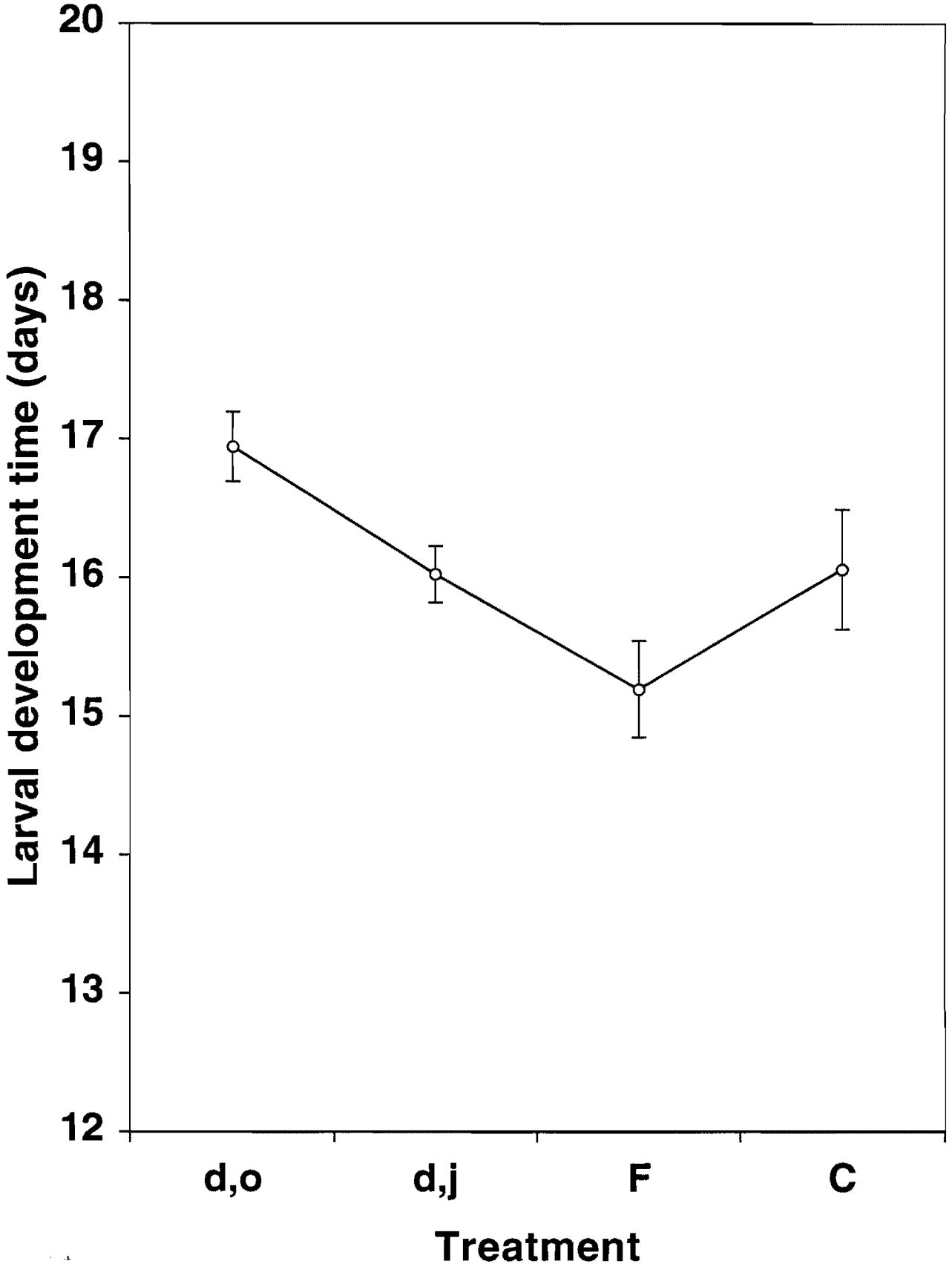
20
19
18
17
16
15
14
13
12
Larval development time (days)
d,o
d,j
F
C
Treatment

Figure 16 a

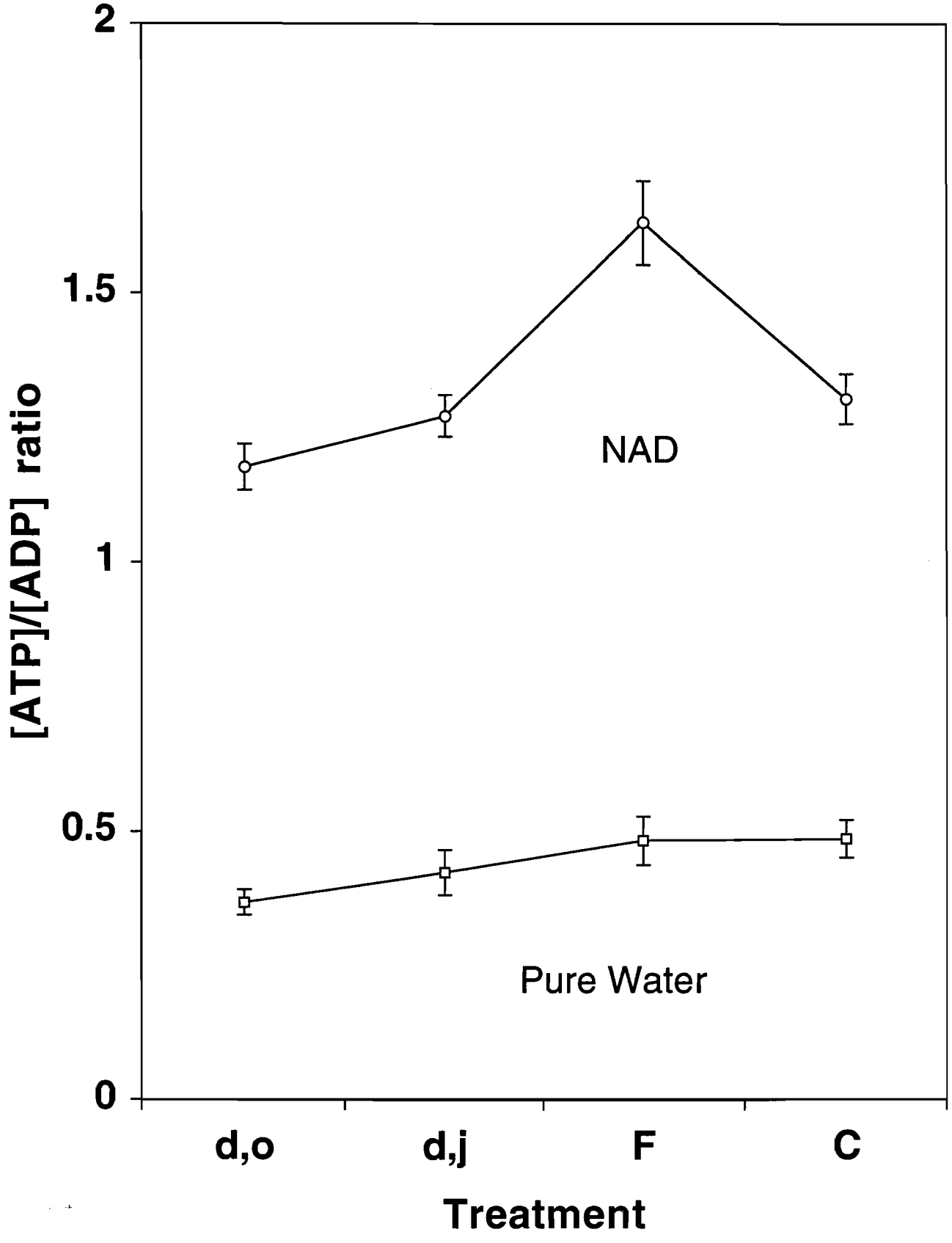

Figure 16 b

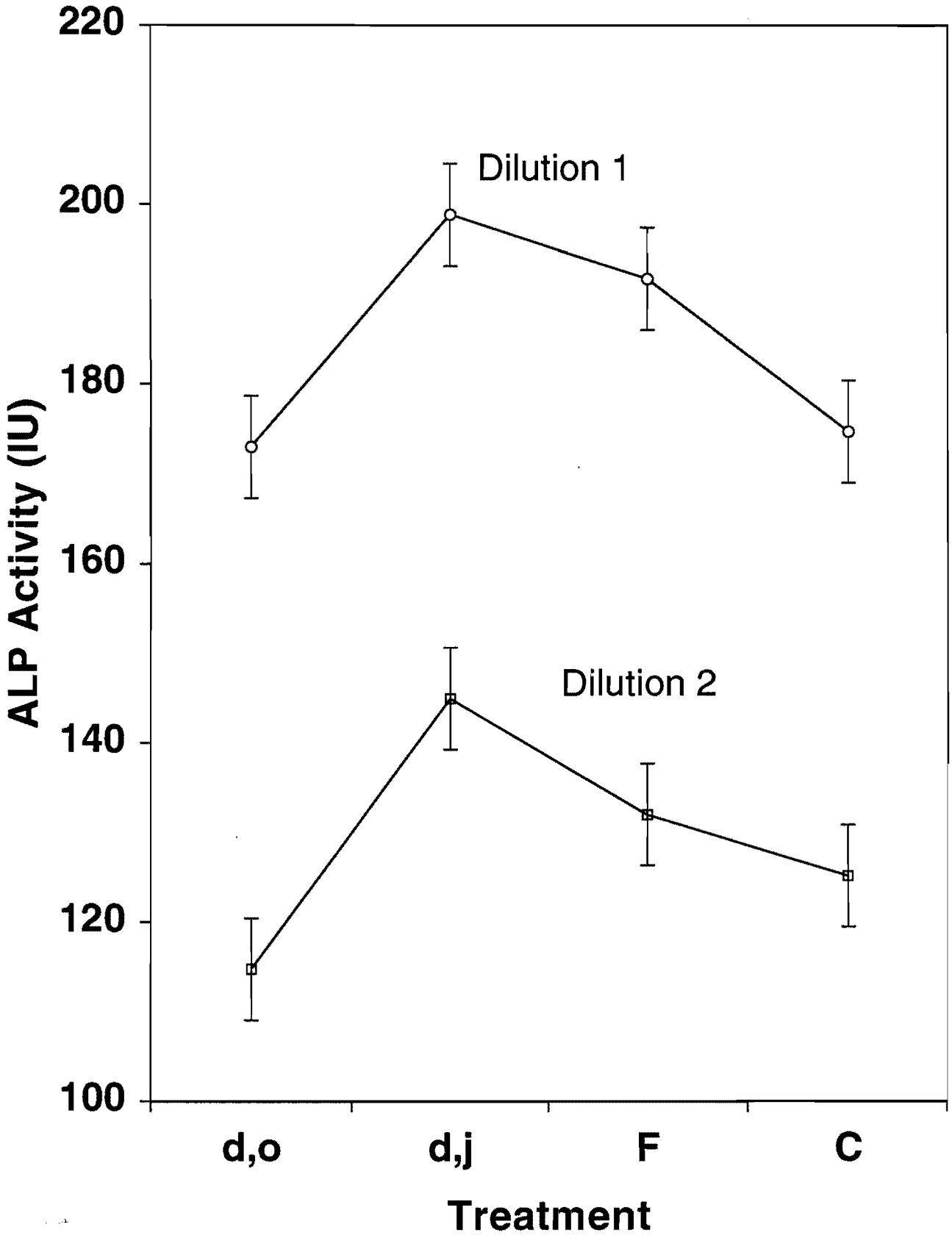
220
200
180
160
140
120
100
ALP Activity (IU)
Dilution 1
Dilution 2
d,o
d,j
F
C
Treatment

Figure 17

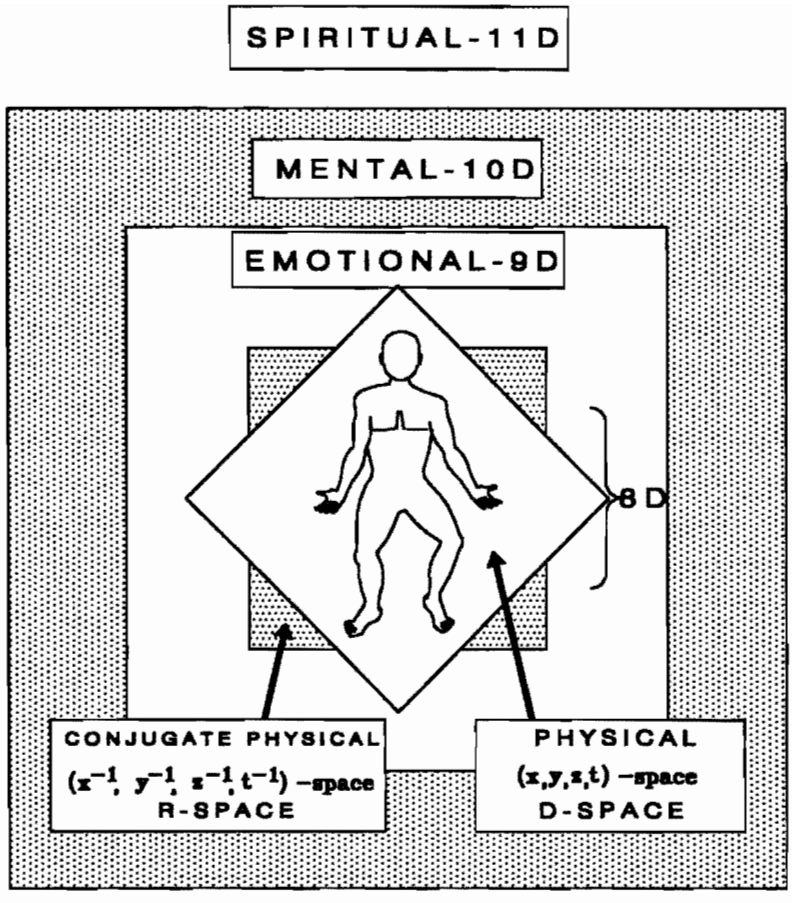

Figure 18

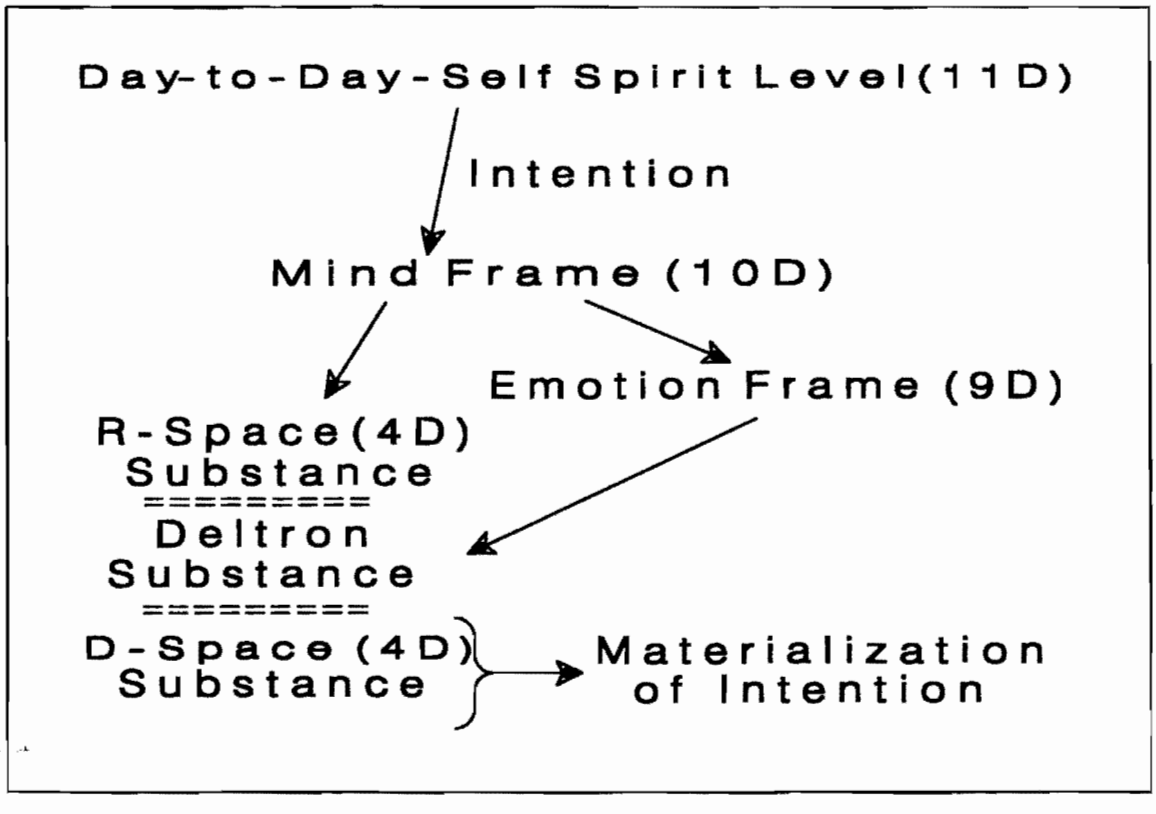

Figure 19